Formation of Perfluorooctane Sulfonate on Suspended Water Droplets via Hydrolyzation of a Volatile Precursor.

A THESIS

SUBMITTED TO THE FACULTY OF THE GRADUATE SCHOOL
OF THE UNIVERSITY OF MINNESOTA

BY

Jeffrey Michael Lanners

IN PARTIAL FULFILLMENT OF THE REQUIREMENTS

FOR THE DEGREE OF

MASTER OF SCIENCE

Matt F. Simcik Advisor

September 2010

Acknowledgements:

I would like to thank everybody who has helped me reach a better understanding of how to design and implement experiments. This research started with a single question and quickly blossomed into an exciting project. Looking back I know I couldn't have done it alone, and I am grateful for everyone who helped me along the way. Specifically I would like to thank the following people. Dr. Matt Simcik -- for his guidance and advice in helping me design experiments to answer some of the questions that came up throughout this research. Joan Manzara – for letting me rant on days when those experiments seemed more frustrating than fun and all the work she did in keeping the lab running smooth as she could. Matt Wogen – For teaching me how to run, and tear apart the LC. Patrick McNamara—for helping motivate me, giving me great advice, and making it fun to work those late nights. Scott Kyser, and Feng-Chih (Timothy) Chang – For the memories and the advice that you were able to provide me. My mom, dad, brothers, and friends – for pushing me and always asking me how my research was coming along. I would also like to thank God for being there through the good and tough times, and helping me learn so much about the world. Last but not least my dear wife Christina Mary Borgen-Lanners – for being patient with me and supporting me throughout the whole process.

Abstract:

Perfluroroctanesulfonate (PFOS) is a ubiquitous global pollutant with no known degradation pathways. A 2001 study by Kannan *et al*. helped to establish PFOS as a global contaminant by measuring it in wildlife and waterways in both remote and urban areas. Atmospheric transport is believed to be the main pathway by which PFOS has been spread globally. The low vapor pressure and high water solubility combine to provide PFOS with a low Henry's Law Constant making direct atmospheric transport unlikely.

One possible explanation for the atmospheric transport of PFOS involves transport and reaction of volatile precursors. Volatile precursors such as perfluorooctane sulfonyl fluoride (POSF) have been demonstrated to react with suspended aerosol water droplets resulting in the formation of PFOS. Underwater exposure of POSF resulted in significantly decreased PFOS production compared to aerosol droplets. This indicates the importance of an air water interface, which allows POSF to position itself so that the reactive sulfonyl head is on the surface of the water and the hydrophobic tail is oriented away.

Experiments involving aprotic solvents indicate the diffusion of POSF into water is faster than simultaneous surface hydrolysis. In order to gain a better understanding of the role the air-water interface plays in PFOS production two parameters were varied independently. The volume of the aerosol droplets exposed and the duration of time they were exposed for was varied in separate experiments. Observations indicate that time

plays a very important role in PFOS production, as longer exposed droplets contained less POSF than those exposed for shorter time periods.

Table of Contents

List of Tables

List of Figures:

List of Equations:

1.1 Overview:

Perfluorinated compounds (PFCs) are a special class of chemicals that contain a carbon backbone which is fully fluorinated, often with a single functional group at one end of the molecule. The functional group added is often a charged moiety such as sulfonic acid or carboxylic acid. These functional groups may be either hydrophilic or oleophilic. Consequently when combined with an insoluble fluorinated carbon tail these compounds serve as excellent surfactants (3M Corporation, 1999). Their unique chemical makeup has lead to difficulty in measurement of some chemical physical parameters including water-octanol partitioning coefficients ($K_{OW)}$. These compounds can range in length from four fully fluorinated carbons (perfluobutanesulfonic acid) to twelve carbons (perfluorododecanoate) or more. Perfluorochemicals have been used in a wide variety of products including food packaging, aqueous firefighting foam, stain repellants, shampoo and insecticides (Giesy, *et al.*, 2002).

1.2 Chemicals of Interest:

This research focuses on two structurally similar perfluorochemicals with vastly different physical properties. The functional group attached to each compound differs slightly and is likely a source of the different physical properties. Perfluorooctanesulfonate (PFOS) is an eight carbon PFC with a sulfonic acid ($-SO_3H$) group attached to one end. The other chemical of interest in this paper Perfluorooctanesulfonyl fluoride (POSF) was the main chemical feedstock used by 3M to produce PFOS. Similar to PFOS, perfluorooctanesulfonyl fluoride is an eight carbon PFC with a sulfonyl group ($-SO_2F$) group on one terminus. The structure of both

compounds can be seen below in Figure 1.

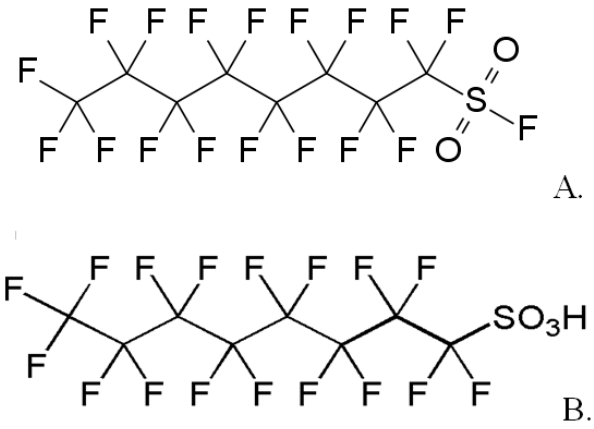

A. Perfluoroctanesulfonyl fluoride (POSF) B. Perfluorooctanesulfonate (PFOS)

Figure 1 Structure of POSF and PFOS.

The carbon-fluorine bonds present in perfluorochemicals are very strong, rendering these compounds resistant to degradation by physical, chemical and biological means (Giesy, *et al.*, 2002). The strength of the carbon-fluorine bond stems from the highly electronegative fluorine atoms inducing a slight polarity on the carbon to which it is bonded (3M Corporation, 1999).

1.3 Physical & Chemical Properties:

Physical –chemical properties for both POSF and PFOS were measured in various laboratory experiments by 3M. Values listed below were determined using the potassium (K^+) salt of PFOS because it was the most ecotoxicologically relevant cation of all PFOS salts produced (Beach, *et al.*, 2006). Also included are values calculated using the EPA's modeling program Estimation Program Interface (EPI) Suite.

Table 1 Physical-Chemical Properties for POSF and PFOS

	POSF	PFOS	Epi Suite POSF	Epi Suite PFOS
Boiling Pt	154 ^{o}C	Not Determined	139^{o}C [d]	229^{o}C [d]
Melting Pt	> 25 ^{o}C	> 400 ^{o}C [a]	--	--
Water Solubility	2.94 E -04 mg/mL [b]	.570 mg/mL [a] - .680 mg/mL [c]	4.25E-9 mg/mL [d]	3.12E-6 mg/mL [d]
Vapor Pressure	213 Pa at 20 ^{o}C [a]	3.31 x 10^{-4} Pa at 20 ^{o}C [a]	767 Pa at 25^{o}C [d]	6.42E-5 Pa at 25 ^{o}C [d]
n-Octanol Solubility	Not Determined	56 mg/L [c]	--	--
Octanol/Water Partion (K_{ow})	Not Determined	Not Determined 3 Phases Formed	--	--

a (3M Company, 2003) b (Ellefson, 2001)

c (Ellefson, 2002) d Values Estimated By EPI Suite (EPA 2010)

Traditionally octanol-water partitioning (K_{OW}) values are established by following guidelines provided by the EPA using what is known as the "Shake Flask Method" (USEPA, 1996). However this wasn't possible with PFOS as its chemical-physical properties caused it to partition between the n-octanol and water phases forming a third insoluble phase (EPA, 2002). Separate solubility measurements of PFOS in both pure water and n-octanol were preformed and used to estimate the K_{OW} at -1.08 in pure water (Ellefson, 2002).

It is worth noting the large difference in the vapor pressure of these two compounds. PFOS has a very low vapor pressure indicating this compound is not likely

to volatilize, while POSF has a vapor pressure six orders of magnitude greater indicating it is much more volatile.

1.4 Toxicology:

Toxicity studies with PFOS conducted on animals have yielded a wide variety of side effects, however little conclusive evidence of adverse effects of PFOS in humans currently exists. A subchronic dosing study preformed on Cyronmoglus monkeys observed increased liver weight, hepatic lesions, weight-loss and lowered levels of triiodothyronine iodine (Seacat, *et al.*, 2002). Other studies have found PFOS to inhibit gap junction intercellular communication (GJIC) in both dolphin and rodent cells (Hu, *et al.*, 2002). Hu *et al*. also found that eight carbon perfluorochemicals such as PFOS were the most proficient in causing GJIC inhibition potentially due to increased cell permeability (Hu, *et al.*, 2003). Gap junction intercellular communication is critical in maintaining homeostasis within cells, therefore PFOS triggered interruption of this process may pose a health risk to mammals (Hu, *et al.*, 2002). Other studies have found PFOS to activate both mouse and human peroxisome proliferator activated receptors (PPAR) (Vanden Heuvel, *et al.*, 2006)

Organofluorines have been observed in human serum since 1968, more recently studies have measured organofluorines in other human matrices including breast milk and umbilical cord blood (Taves, 1968, Ehresman, *et al.*, 2007, Apelberg, *et al.*, 2007). Although it has long been observed in humans, few studies have found convincing evidence of PFOS causing degenerate health effects in humans. A 2003 study of 3M

employees involved in PFOS manufacturing found a positive association between PFOS and elevated levels of the thyroidal hormone T3 (Olsen, *et al.*, 2003). However this finding was disregarded as being irrelevant as it differed from an earlier mentioned study by Seccat *et al*. which found decreased thyroid hormone levels in monkeys (Olsen, *et al.*, 2003, Seacat, *et al.*, 2002). An increased incidence of bladder cancer caused mortality was observed in workers with high levels of exposure to POSF based materials. Some scientists feel this observance isn't conclusively linked to perfluorochemical exposure as there are no reported incidents of bladder cancer in high dose long term animal studies (Olsen, *et al.*, 2003).

1.5 Environmental Concerns:

Although some scientists don't feel PFOS represents a threat to human health, there is still cause for concern (Olsen *et al.*, 2003). PFOS remains a global pollutant resistant to degradation nearly a decade after 3M ceased production. The high energy carbon fluorine bonds found in PFOS prevent this compound from being degraded in nature via chemical (3M Company, 2001), biological, (STS Conslutants, Ltd, 2007) and photolytic (3M Company, 2001) processes. PFOS has been shown to be both bioaccumaltive and ubiquitous throughout the global environment (Giesy, *et al.*, 2001).

Transport of chemicals throughout the environment is governed by many processes and a few basic physical-chemical properties. Long range atmospheric transport is governed primarily by a chemical's Henry's Law Constant and vapor pressure. The Henry's Law Constant of a compound is useful in establishing the extent

to which a compound will partition between air and water. Compounds with low Henry's Law Constants tend to partition to water in the atmosphere or terrestrial surface water and remain there (Simcik, 2005). As a result compounds with low Henry's Law Constants are more likely to partition to water and be washed out of the atmosphere.

The vapor pressure of a compound determines the likelihood a compound will volatilize and whether an atmospheric compound is likely to be found as a gas or associated with particles (Simcik, 2005). The atmospheric state of a compound plays a profound role in long range atmospheric transport as large particles are likely to settle out of the atmosphere faster than small particles and all particles are more easily scavenged by precipitation than gases (Simcik, 2005). The low vapor pressure of PFOS makes it more likely to associate with particles in the atmosphere. POSF has a higher vapor pressure and is more likely to remain as a gas in the atmosphere.

The reported solubility and vapor pressure as seen above in Table 1 can be used to estimate Henry's Law Constants for PFOS and POSF. Henry's Law Constant values have been reported and estimated for PFOS, but not for POSF. Henry's Law Constants were estimated using literature values to determine how these compounds would behave in an air water environment. The output provided by the EPA software EPI Suite included an estimate of Henry's Law Constants for both POSF and PFOS which was compared to the literature calculated values. The values estimated by EPI Suite are higher than other calculated values for both PFOS, and POSF. This estimated difference was smaller when chemical-physical values were entered into EPI Suite. Henry's Law

Constants obtained from EPI Suite and literature calculated values can be seen below in Table 2.

Table 2 Henry's Law Constants for PFOS and POSF

Compound	Calculated Value	EPI Suite Value	EPI Suite with User Entered Values
PFOS	3.05E-9 atm-m^3/mol[a]	1.10 E-2 atm-m^3/mol	2.86 E-9 atm-m^3/mol
POSF	22.5 atm-m^3/mol[b]	67.9 atm-m^3/mol	22.5 atm-m^3/mol

a (3M Company, 2003)

b Calculated using literature values from Table 1.

As can be seen above in Table 2 the Henry's Law Constants for POSF are much larger than PFOS. The large Henry's Law Constant arises from the combination of a high vapor pressure and low water solubility. This indicates POSF will more likely partition away from water toward air, consequently making POSF less likely to be washed from the atmosphere. Additionally the high vapor pressure indicates that POSF is a volatile compound. Experiments were designed to take advantage of the volatile nature of POSF, it was theorized that POSF would hydrolyze to form other perfluorochemicals in the presence of an aerosolized water droplet. Comparatively PFOS has a low vapor pressure and high water solubility, which makes it unlikely to undergo volatilization and long range atmospheric transport.

1.6 Fate and Transport:

Though its chemical properties predict that it should remain stationary, PFOS has been observed to be a global pollutant. Studies have measured PFOS in wildlife (Giesy, *et al.*, 2001, Kannan, *et al.*, 2001, Verreault, *et al.*, 2007, Tomy, *et al.*, 2004, Smithwick,

et al., 2006), humans (Dallaire, *et al.,* 2009, So, *et al.,* 2006), freshwater (Simcik, and Dorweiler, 2006), and oceans (Ahrens, *et al.,* 2009). Many of the same studies that measured PFOS in wildlife observed increasing concentrations associated with higher trophic level predators indicating that PFOS can both bioaccumlate and biomagnify (Giesy, *et al.,* 2001, Kelly, *et al.,* 2009).

A study measuring both PFCs and polychlorinated biphenyl congeners (PCBs) in polar bears found a positive correlation between the two chemical classes, indicating similar source regions and transport pathways for PFCs and PCBS (Smithwick, *et al.,* 2005). A 2005 study found PFOS in isolated remote lakes in northern Minnesota where the only expected source was atmospheric deposition (Simcik, *et al.,* 2005). The observed short doubling times of PFOS in different species of wildlife in the Canadian Arctic (5.8-10 years) also implicate atmospheric transport as the most likely transport pathway to this region, as oceanic transport would take longer (Butt, *et al.,* 2007, Smithwick, *et al.,* 2006). These short doubling times coincide well with the estimated POSF production doubling time estimated at 3-13 years (Paul, *et al.,* 2009).

Due to its low vapor pressure it is unlikely for PFOS to undergo atmospheric transport, hence a common theory is that volatile precursors are transported atmospherically and react to from PFOS. Studies have measured volatile PFOS precursor compounds such as N-methyl and N-Ethyl perfluorooctane sulfonamidoethanol, and N-ethyl perfluorooctane sulfonamide throughout the globe (Lowen, *et al.,* 2008, Stock, *et al.,* 2004, Martin, *et al.,* 2002).

A 2006 experiment by D'Eon *et al*. observed that reactions of ·OH radicals with four carbon perfluorochemicals such as N-methyl perfluorobutane sulfonamidoethanol (NMeFBSE) would produce small amounts of perfluorobutane sulfonic acid (PFBS) (D'Eon, *et al.*, 2006). This experiment presented a pathway which may explain how corresponding eight carbon N-methyl perfluorooctane sulfonamidoethanol (N-MEFOSE) could react to form PFOS. N-MEFOSE is more volatile than PFOS and was produced in large quantities for many years until the phase out of POSF based products in 2002. However there has been little evidence of this reaction occurring in the natural environment. Contrary to D'Eon et. al. PFOS production was not observed in an aqueous solution in which suspected precursor chemicals such as N-ethyl perfluorooctane sulfonamidoethanol, underwent indirect photolysis by ·OH radicals (Plumlee, *et al.*, 2009). Measurements of PFOS and other perfluorochemicals in oceans throughout the world indicate that PFCS are likely transported via currents to remote locations (Yamashita, *et al.*, 2004, Ahrens, *et al.*, 2009).

1.7 Production and Synthesis:

Historically PFOS was synthesized from a series of reactions starting with the feedstock chemical POSF. POSF production occurs via a process known as Simmons Electro-Chemical Fluorination (ECF). In this method a feedstock compound 1-Octanesulfonyl Fluoride is dispersed in liquid anhydrous hydrogen fluoride and an electrical current is passed through the solution. This results in hydrogen atoms on the organic feedstock being replaced by fluorine (3M Corporation, 1999). The reaction and starting materials are shown below in Figure 2.

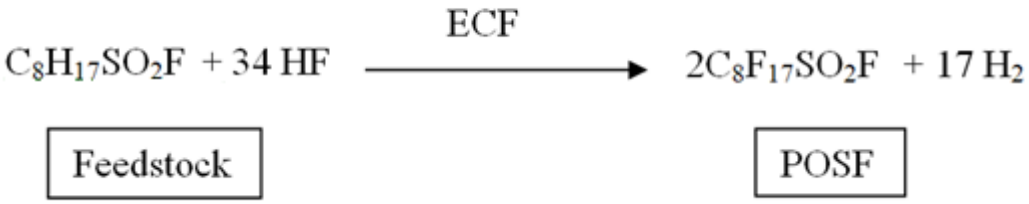

Figure 2 Electrochemical Fluorination Process to Produce POSF

The commercial ECF process produces approximately 70% linear POSF isomers and 30% branched homologues and other byproducts (3M Corporation, 1999). Commercial PFOS production began in 1949 on a small scale, but quickly increased in 1972 due to improved commercial demand. This production increase continued until its peak in 1999 and rapidly declined when 3M announced a phase out in 2000 (Paul, *et al.,* 2009).

According to Paul *et al*. (2009), more than 600 steps were required to transform POSF to its various useable end products. Due to the large number of steps it is likely that some POSF was lost throughout the process. Prior to phase out of POSF, 3M stated that there were over 80 unmonitored venting points in the equipment used to make sulfonated perfluorochemicals (3M Company, 2003). Fugitive emissions of POSF which volatilize to the atmosphere would likely provide a source of volatile reactive PFOS precursors.

1.8 Phase out and Evidence for Atmospheric Transport:

Temporal trend studies observed the phase out of PFOS as a rapid decrease in PFC concentrations in animals from the Canadian Arctic (Hart, *et al.,* 2009, Butt, *et al.,* 2007). This rapid decrease was likely caused by the cessation of POSF production resulting in decreased volatile PFOS precursors. Other studies observed PFOS

concentrations in seals and polar bears of Greenland continued to increase since the phase out occurred in 2002 (Dietz, *et al.*, 2008, Bosi, *et al.*, 2005). The decrease associated with ringed seals in the Canadian Arctic is indicative of an atmospheric transport pathway while the increasing concentrations in Greenland indicate a slower transport pathway such as oceanic currents (Armitage, *et al.*, 2009).

Though these studies present evidence of atmospheric transport to remote regions, the formation pathway of atmospheric PFOS is not completely understood. Studies such as D'Eon *et al*. have focused on volatile precursors such as N-MEFOSE reacting in the gaseous phase as an explanation for the atmospheric transport of PFOS. The work done by D'Eon, has resulted in few other volatile precursors including POSF being examined as playing a potential role in the transport of PFOS. Similarly research has focused on reactions of precursors in either the gaseous phase or in a bulk water solution. Few experiments have been designed to determine how these surfactants behave in other environments. Specifically how these chemicals may react on the surface of smaller airborne water droplets or other atmospheric particles.

In order to gain a broader understanding of how smaller surfaces may affect PFOS production, POSF was allowed to volatilize in a sealed container with a suspended aerosol water droplet. Similar to D'Eon *et al*. and Martian *et al*., the research preformed herein demonstrates that volatile compounds are likely responsible for the formation of PFOS. However the physical-chemical properties of volatile precursors make it unlikely that gas phase reactions are responsible for all atmospheric PFOS. It is more likely that

reactions of volatile precursors occur on the surface of an intermediate such as aerosols or other fine particles.

In 2008 McMurdo et. al. studied the formation of perfluorooctanoic acid (PFOA) as it related to aerosol droplets. This study found aerosol droplets could be enriched with perfluorooctanoate (PFO) which would then be protonated on the droplets surface to form gaseous PFOA (McMurdo, *et al.,* 2008). This mechanism may be responsible for some of the observed atmospheric transport and formation of PFOA in remote regions such as the Arctic. (McMurdo, *et al.,* 2008). PFOA is an eight carbon non-volatile perfluorochemical like PFOS, and has also been shown to have a global distribution. It may be possible that PFOS is formed through a similar mechanism on the surface of aerosol droplets by hydrolysis of a volatile precursor.

1.9 Thesis Objective:

This thesis will present unique findings on the behavior of PFOS and its main chemical feedstock POSF as observed in an atmospheric aerosol environment and how they relate to global contamination. Initially a novel method for creation of PFOS in an atmospheric aerosol environment will be described. Data collected from these experiments yielded an array of information which was used to better understand some of the physical and chemical processes that POSF may undergo in the environment. An attempt was made to compare hydrolysis rates of POSF in a bulk interface to rates on an aerosol of the same solution. Additionally new insight was gained into how the surfactant properties of POSF affect its hydrolysis in both aerosol environments and the bulk interface.

2. Methods Section:

2.1 Syringe and Vial Preparation.

Prior to sample creation four 10 µL syringes (Hamilton #701, Reno, NV) were cleaned as outlined below. A small amount of the following solvents; Optima grade methanol (Fisher Scientific, Fair Lawn, NJ) Omnisolv acetonitrile (EMD, Gibbstown, NJ) and HPLC grade dichloromethane (Honeywell, Muskegon, MI) was applied to separate Kimwipes which were used to wipe all needles and syringe bores three times. After wiping, the syringes were reassembled and flushed 30 times with a new beaker of clean solvent in the same order. In order to assure the syringes were clean separate 300 µL glass inserts were filled with clean acetonitrile using the assembled syringes. These inserts were placed into large mouth screwcap glass autosampler vials (Chromtech, Apple Valley, MN) and analyzed to determine if any residual PFOS remained in the syringes. The syringes and needles were then disassembled and air dried overnight. Two 40 mL amber screw cap vials (Chromtech, Apple Valley, MN) were also cleaned by rinsing three times with clean solvent in the order listed above. Afterwards these vials were baked out in a muffle furnace at 450 ^{o}C for 6 hours to burn off any remaining solvents or compounds.

2.2 Headspace Sampling.

Sampling was modified from a method developed by Nam-Sun Kim *et al.* and Mi-Jin Jung *et al.* (2005, 2006).

One cleaned 40 mL vial was placed in a fume hood and 200 µL of POSF (Aldrich, Milwaukee, WI) was placed into the bottom of the vial via Drummond pipette. Special care was taken to ensure all the POSF was placed on the bottom of the vial and that the vial was not disturbed. This included clamping the vial to a ring stand prior to insertion of POSF and avoiding touching the sides of the vial when the POSF was placed into the vial. After the POSF was placed in the vial a screw cap and viton septum were secured on top of the vial. The POSF in the bottom of the vial was allowed to volatilize for up to 24 hours to saturate the headspace of the vial. The air temperature inside the vials was assumed to be equivalent to ambient air temperatures measured in the lab at 19 ^{o}C. A depiction of the experimental setup described above can be seen below in Figure 3.

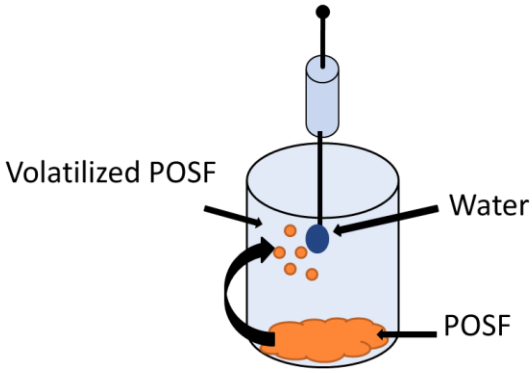

Figure 3 Suspended Water Droplet Air Exposure Experiment

Prior to headspace exposure, the syringes were flushed 10 times with reverse osmosis (R.O.) water to remove any solvent remaining in the syringes. Following the final rinse, one microliter of R.O water was drawn up into each syringe for exposure. Three of the syringes were labeled 1- 3 and the fourth syringe was labeled Blank in order

to minimize contamination of the blank syringe. The numbered syringes were used to pierce the septum of the vial containing POSF. The plungers were depressed suspending a one microliter water droplet from the tip of the needle. Simultaneously the blank syringe was inserted into an empty 40 mL vial and a one microliter droplet of water was exposed for one hour. All syringes were inserted into the vials to the full extent of the needle thus ensuring near uniform height above the liquid POSF during each experiment.

After the water droplets were exposed for one hour the water droplets were pulled back up into the syringe and each droplet was placed into a separate 300 µL glass insert (Chromtech, Apple Valley, MN) filled with 250 µL of methanol. After the droplets were expunged into methanol the syringes were flushed 20 times with methanol from the insert to help ensure transfer of water and PFOS from the syringe. Each insert was placed into a two mL screw cap autosampler vial, and then secured with a screw cap and viton septum (Chromtech Apple Valley MN).

2.3 Selection of Column for Liquid Chromatography:

Chromatographic separation of compounds was initially achieved using a narrow bore Phenomenex Luna B2 C_{18} analytical column(50mm x 1mm, 5µL) attached to a pre-filter guard column (Security Guard, C_{18}, Phenomenex, Torrance, CA). Additionally a two solvent mobile phase was employed to aid in chromatographic separations. The aqueous portion of the mobile phase (Solvent A) consisted of 2 mM ammonium acetate (Sigma, Milwaukee, WI) dissolved in a mixture of 70:30 (V: V) R.O. water, and Optima grade methanol (Fisher Scientific, Fair Lawn, NJ). The organic portion of the mobile

phase (Solvent B) was composed of 2 mM ammonium acetate dissolved in 100% Optima grade methanol (Fisher Scientific, Fair Lawn, NJ). Prior to sample analysis solvents were degassed by bubbling nitrogen through them for 10 minutes.

The column was conditioned by slowly increasing the flow rate of solvent A until the method flow rate was reached. Small volume samples (1 µL) were injected onto the column for analysis. The mobile phase started out with 100 % solvent A being pumped through the lines and was slowly changed over to a mixture containing 57.1 % B during the first 13 minutes of the run. The flow was then held at this ratio for five minutes and then changed over to 100 % B until the run had occurred for 33 minutes. The column was then maintained at 100 % B until 36 minutes and then switched to 100 % A at 37 minutes where it was held for eight minutes to re-equilibrate the column prior to the next injection. The flow rate was held constant at 50 µL/min, and the temperature of the column was held at 38 ^{o}C throughout the run.

2.3.1 Second Column:

Large variability in the amount of PFOS produced on each droplet created speculation that methanol in the experiment was causing hydrolysis of any unreacted POSF on the water droplets surface. This was later confirmed and will be discussed shortly. A new method was developed and methanol in the system was replaced with acetonitrile. Solvent A was switched to a mixture of 70 % reverse osmosis water and 30 % (V: V) Omnisolv grade acetonitrile (EMD, Gibbstown, NJ) and buffered with 2 mM ammonium acetate (Sigma -Aldrich, Milwaukee, WI). Solvent B was replaced with 100

% acetonitrile and left unbuffered. The column was exchanged for a Betasil C_{18} (50 mm x 2 mm, 3µm, Thermo-Hypersil, Keystone; Bellefonte, PA). This column had been shown to be effective in separating perfluoro compounds using a water acetonitrile mobile phase in work performed by Inoue *et al*. (2004). After several attempts a method was designed that allowed acceptable separation of a perfluorochemical calibration standard containing perfluorochemicals ranging from C6 to C12.

The new gradient started at 100% solvent A and was switched to 22 % solvent B over the first 8 minutes. This mixture was maintained until 28 minutes, and was then switched over to 100% A over the course of a minute. It was then held at 100% A until 36 minutes to allow the column to re-equilibrate. The flow rate was increased to 200 µL/min and the sample volume withdrawn was increased to 10 µL. Prior to running experiments solvents were degassed and filtered and the column was conditioned as described earlier.

After running multiple experiments in which significant increases in PFOS concentrations were observed between droplets an assumption was made that the water in Solvent A was causing additional hydrolysis of unreacted POSF as it moved through the column. This observation led to the creation of a third method.

2.3.2 Isocratic Analysis:

The third method used to analyze droplets for this experiment involved using only one solvent. Samples were prepared as in the previous methods using acetonitrile as the organic and only solvent. Since the organic phase is typically used to push these

compounds off of the column an isocratic system of purely organic solvent would result in very little sample retention. Due to the lack of sample retention the use of a column was eliminated from the system. The solvent gradient started as 100% B and was maintained for four minutes to make sure that all of the compounds were pushed through the lines. Four solvent blanks were injected between each sample to clean the lines and injection needle. Samples were analyzed multiple times over the course of 48 hours to observe in solution hydrolysis. The flow rate for the new method was maintained at 200 µL/min, and the temperature, and injection volume remained the same as the previous method 38 ^{o}C and 10 µL respectively.

2.4 Preparation of solvents.

Prior to every experiment the solvents were filtered twice through a .2 µm polycarbonate filter (Millipore, Eschborn, Germany) in order to remove any particulates that could impede flow of solvent through the lines. Afterwards solvents were degassed on the LC by bubbling nitrogen through them for 15 minutes. Following sample analysis the column and lines were flushed with non-buffered solvents to prevent bacterial growth and residual buffer buildup.

2.5 Mass Spectrometry.

Compounds were detected in each method via a Hewlett Packard 1100 series mass spectrometer (M.S.) operated in negative electrospray mode. Prior to running samples, the MS was tuned. Tuning was considered to be acceptable when signals of the tuning masses were $\geq$ 8000. If the tune signals were lower than this level, M.S was

autotuned or subjected to manual optimization of tuning parameters. The spray chamber was also examined and if necessary cleaned and polished. Important parameters for the M.S. were held constant and can be seen below in Table 3.

Table 3 Important Mass Spectrometer Parameters

Capillary Voltage	70 V
Fragmenter Voltage	4000 V
Drying Gas Flow Rate	8 L/ min
Drying Gas Temperature	300^{o}C
Quadropole Temperature	100^{o}C

The detector was operated in Selective Ion Monitoring (S.I.M) mode. In this mode each analyte is detected by the [M^-] ion which can be seen in Table 4 below.

Table 4 Molecular Ions Detected in Experiments

Compound	Formula	Ion in Negative Mode
PFOS	$CF_3(CF_2)_7SO_3^-$	499
POSF	$CF_3(CF_2)_7SO2^-$	483

For this experiment the parent ion for PFOS was 499 and the parent ion for POSF was 503.

2.6 Sample Quantification:

Samples were quantified using both internal and external standards. In experiments where methanol was used, a known amount of [$^{13}C_4$]-PFOS was added to samples as an internal standard via Drummond pippet.. The mass of PFOS produced in each sample can then be calculated by comparing the area of the internal standard to a Relative Response Factor (RRF). The RRF is calculated by placing a known amount of internal standard into a standard with a known amount of unlabeled compound and

dividing the mass to area ratios of both labeled and unlabeled compounds. An example can be seen below as Equation 1.

$$RRF = \frac{\text{Mass of Analyate}}{\text{Peak Area}} \div \frac{Mass\ of\ Internal\ Standard}{Peak\ area\ of\ Internal\ Standard}$$

Equation 1 Example of Relative Response Factor for Calculations

The RRF calculated from this equation can then be applied to samples where the PFOS concentration is unknown, an example can be seen below in Equation 2.

$$Mass\ of\ Unknown\ Sample = Area\ of\ Unknown\ Analyte * RRF\left(\frac{Mi}{Ai}\right)$$

Equation 2 Calculation of PFOS in Unknown Sample Using Relative Response Factor

In order to find the mass in the unknown samples the mass of the internal standard added to each sample (*Mi*) is divided by the area of the internal standard in that sample (*Ai*) this value is multiplied by the RRF and again by the area of the unknown sample. This method wasn't applied to samples that didn't already contain methanol because the internal standard was stored in methanol and would hydrolyze unreacted POSF. When samples were prepared without methanol an external calibration curve was used to quantify samples.

A five point external calibration curve was used to quantify samples in experiments where droplets were placed in acetonitrile. External calibration standards were chosen based on previously observed PFOS concentrations in methanol experiments. Based on these results it was expected that PFOS samples in aprotic

solvents should be present in lower concentrations. PFOS calibration solutions were made in Optima grade methanol (Fisher Scientific, Fair Lawn, NJ) and included concentrations of 5, 25, 50, 100, and 250 ng/mL. Separate autosampler vials were made for each standard which were analyzed on the LC-MS. A calibration curve was then constructed using Microsoft Excel. Linear regression for the calibration curves was performed using Excel. Regression lines were not forced through the origin. R^2 values were typically above .99, though some r^2 values were as low as .95. Using the slope of the line calculated by Excel the mass of PFOS in unknown samples was calculated.

2.7 Quality Assurance & Quality Control:

A blank for each experiment was created by exposing a water droplet to a separate empty sealed vial while droplets were exposed to POSF. The blank was processed using the same procedures as droplets exposed to POSF including addition of internal standards. After each sample the syringes were cleaned as described earlier. Part of the cleaning process included using the cleaned syringes to fill a 300 µL insert with acetonitrile or methanol depending on the experiment. These inserts were than analyzed for PFOS and POSF using the LC-MS to ensure there was no carryover between experiments. A similar check was preformed while samples were analyzed on the LC-MS. In order to ensure that PFOS detected in each sample was not the result of carryover a solvent blank was ran between each sample. Additional procedures were taken to verify that the instrument response was uniform throughout the sequence. One way to determine if the response was uniform was the repeated running of calibration standards

after every 6 samples throughout the sequence. These calibration standards were then compared afterwards to see if there was any change in the mass detected by the M.S.

2.8 Additional Exposure Experiments:

Other experiments were conducted in order to gain a better understanding of how the hydrolysis rates of POSF in a bulk solution compares to the rates observed on an aerosol droplet. In these bulk experiments autosampler vials were cleaned as previously described. Afterwards a known volume of water either one or two milliliters was added to each container and a known amount of neat POSF ranging from 1 to 3 µL was added to the center of the water via syringe. The pH of R.O. water used was determined to be at 5.85 at 19.2 ^{o}C prior to POSF exposure and was not measured after exposure. The vials were then analyzed on the LC-MS using the second method described. Quantification of these samples occurred via an external calibration curve. A depiction of the experimental setup described above can be seen Appendix B.

Another set of experiments was designed in an attempt to determine how surface area affected PFOS production. One microliter droplets of POSF were suspended above different sized containers of water, via syringe and allowed to volatilize for 10 minutes. Afterwards the syringe and POSF were removed and 300 µl of sample was placed into an insert and analyzed. A depiction of this experimental setup can be seen in Appendix B.

3.0 Results and Discussion:

The experiments described earlier demonstrate for the first time the laboratory synthesis of PFOS on a suspended aerosol water droplet. A depiction of the hydrolysis reaction responsible for PFOS formation can be seen below in Figure 4.

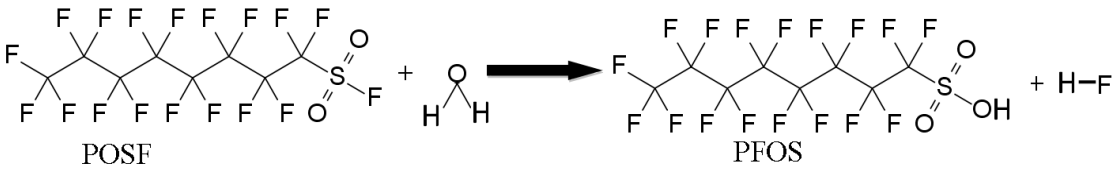

Figure 4 Hydrolysis Reaction to Produce PFOS

The volatile, PFOS-precursor POSF was shown to hydrolyze and form significant amounts of PFOS on the surface of suspended water droplets. POSF exposed underwater for 10 minutes, was observed to produce PFOS in smaller quantities than on an aerosol droplet. Smaller amounts of PFOS were also observed in experiments where POSF was suspended above water for 10 minutes, and allowed to hydrolyze on the water's surface. The averaged amount (N = 3) of PFOS produced in underwater and above water experiments can be seen below in Figure 5. Standard error was calculated and is represented by error bars in the Figure 5. PFOS production on suspended water droplets was not included in Figure 5, as the experimental conditions varied from those in other experiments.

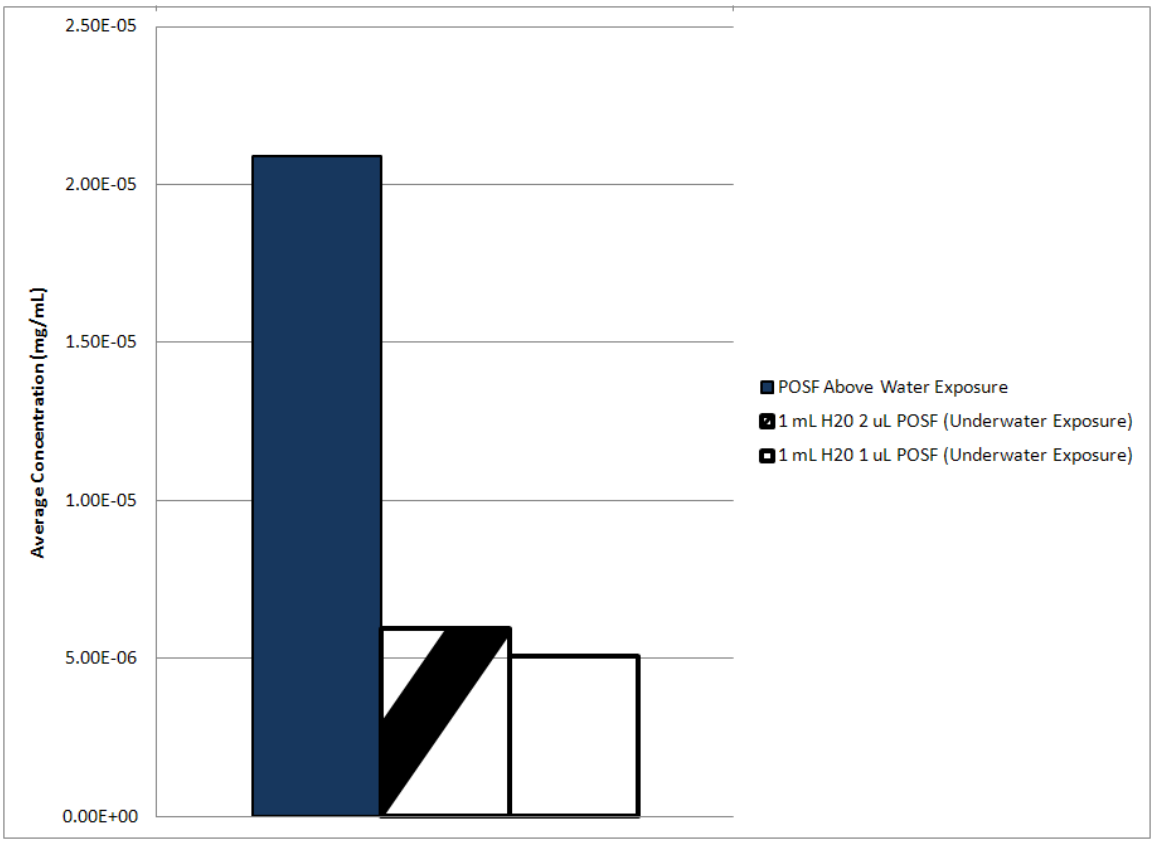

Figure 5 Average PFOS Production After 10 Minute Exposure.

As can be seen in Figure 5, PFOS production is greater when POSF is allowed to volatilize and react on the water surface. This disparity in PFOS formation indicates the importance of the air-water interface in the reaction and formation of these surfactant molecules.

Due to the surfactant nature of POSF it can be expected that the air-water interface would play a significant role in the formation of PFOS. The hydrophobic fluorinated tail of POSF plays a significant role in PFOS production. When the gaseous form of this molecule comes into contact with water the tail of the molecule is likely to be oriented outwards into the air, away from water. This orientation results in the

reactive sulfonyl fluoride (-SO_2F) being exposed to water and consequently undergoing hydrolysis to form PFOS. A depiction of how the orientation influences production can be seen below in Figure 6.

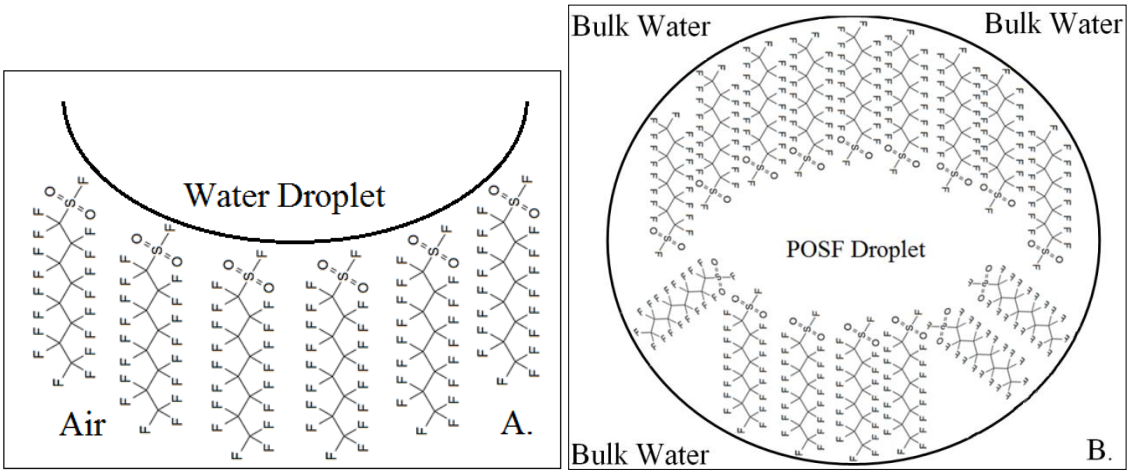

A. POSF oriented with the reactive sulfonyl group toward the water surface on a suspended water droplet. B. POSF oriented with the reactive sulfonyl head group inward, away from water, in an underwater exposure experiment.

Figure 6 Orientation of PFOS in Different Exposure Settings

As described earlier when POSF was placed directly into water, the amount of PFOS produced was greatly reduced compared to the amount formed on an aerosol droplet. As seen above in Figure 6, when immersed in water POSF formed PFOS in concentrations averaging less than two nanograms per milliliter. The low yield in the immersion exposure was not entirely unexpected due to the low water solubility of POSF. Studies by Ellefson found the solubility of POSF in water to be less than 294 ng/mL (Ellefson, 2001).

The reduction in PFOS formation can be attributed to the lack of an air water interface which results in POSF adapting a less reactive orientation. When placed

directly into water, POSF forms something of a micelle in which the reactive sulfonyl groups are forced toward the center and the unreactive tails are oriented outwards in a spherical shape. The larger fluorinated tails exhibit a stronger effect on the molecules' orientation, forcing the smaller sulfonyl head group inwards in a slightly less favorable confirmation. The hydrophobic fluorinated tails are likely closely packed together, as it presents a more favorable environment than being surrounded by water.

The slight negative charge on the tail which results from the electron withdrawing fluorines may also play an important role in explaining this unreactive POSF sphere on the bottom of the containers. If the tails were packed close enough together they would effectively function as one very large negative ion which would likely appear as a pocket of POSF surrounded by water. Whether it is caused by a large cavity to support a negative ion or the dense packing of hydrophobic tails the formation of a POSF micelle demonstrates the importance of the air-water interface in the hydrolysis of POSF to PFOS. The lack of an air water interface prevents POSF from arranging its orientation so that the hydrophobic tail doesn't have to interact with water.

POSF appears to partition into the droplet at a faster rate than it is able to hydrolyze on the droplets surface, a fact which was not readily evident in initial experiments. While it was not possible to directly determine of the rates for each process, data collected from experiments indicates all of the POSF doesn't immediately react upon contact with the aerosol droplets surface. The four main processes that govern aerosol PFOS formation are depicted in Figure 7 below.

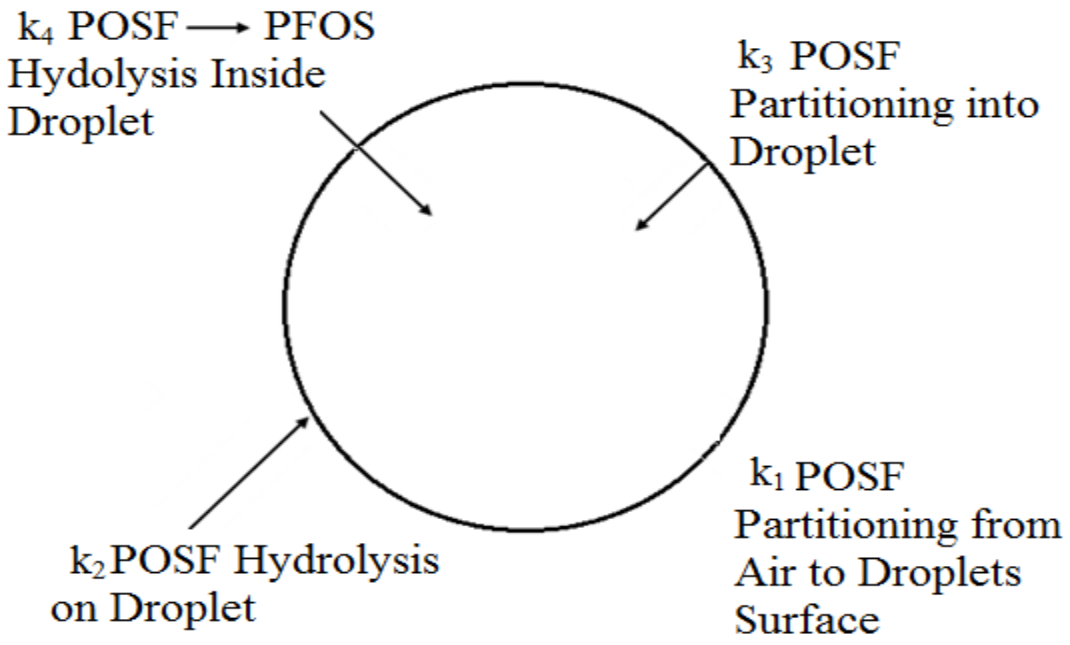

Figure 7 Processes that Govern Formation of PFOS on an Aerosol Droplet

When exposed droplets are stored in methanol prior to analysis, any unreacted POSF is rapidly hydrolyzed to PFOS. The use of the aprotic solvent acetonitrile proved beneficial in determining POSF wasn't instantly hydrolyzed on the surface of the aerosol droplet. Samples placed in acetonitrile were analyzed multiple times over the course of a 48 hour period. Initial concentrations were small ranging between two and five ng/mL. However subsequent examinations produced higher concentrations as time progressed as can be seen below in Figure 8.

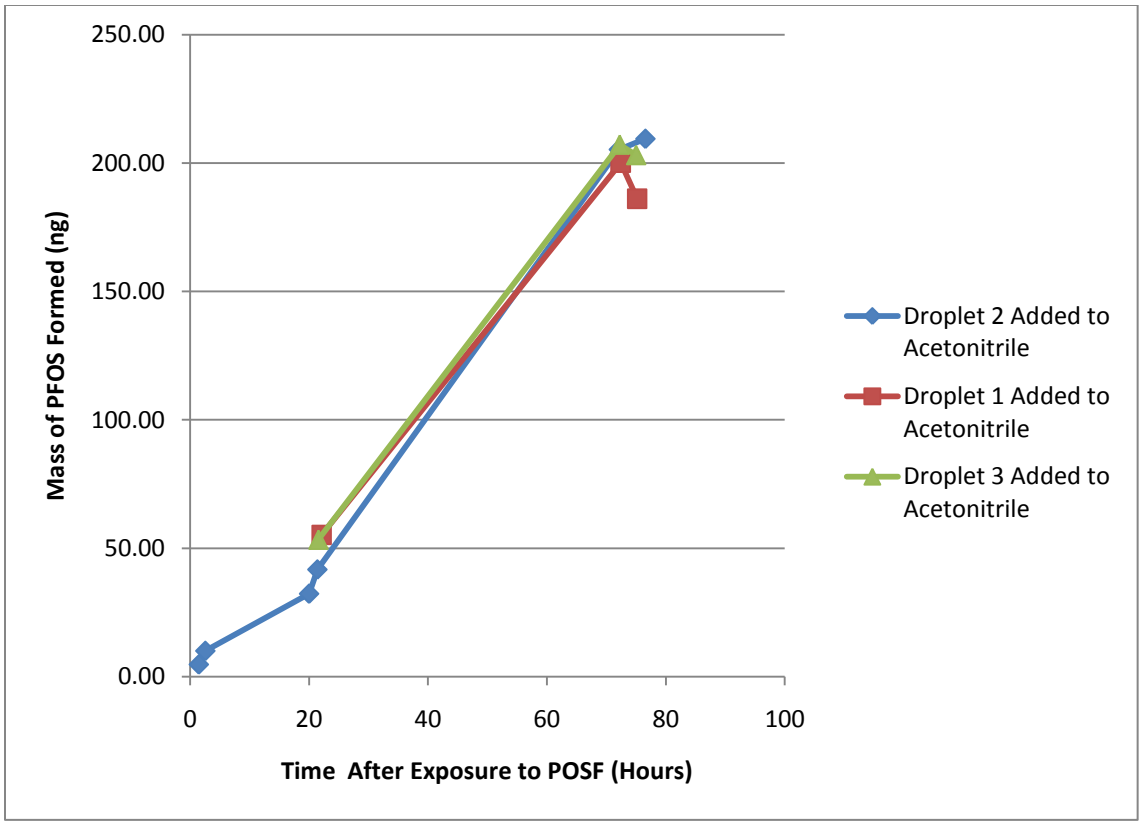

Figure 8 Change in PFOS Formed Over Time for Droplets Added to Acetonitrile

Repeated analysis of autosampler vials indicated an increase in the amount of PFOS formed after droplets were placed into vials. This increase is likely attributed to water in the container being scavenged by unreacted POSF. As seen above in Figure 8 this phenomenon appears to be time dependent, due to the fact that vials sampled multiple times had comparable concentrations to those analyzed once at a similar time point. Additional data demonstrating this can be seen in Appendix C.

The sole source of hydrolysis responsible for the PFOS increase in acetonitrile is the water from the droplet which was dispersed upon entering acetonitrile. As the POSF, which previously partitioned into the aerosol droplet, came into contact with water it was hydrolyzed, slowly increasing the amount of PFOS present. Direct determination of an in

solution hydrolysis rate wasn't possible, as the initial PFOS concentration on the droplets prior to placement in the solvent couldn't be determined.

When water droplets were placed into methanol the temporal effect on concentration was much different. Exposed droplets placed in methanol demonstrated a higher concentration of PFOS that was independent of time after exposure (Figure 9).

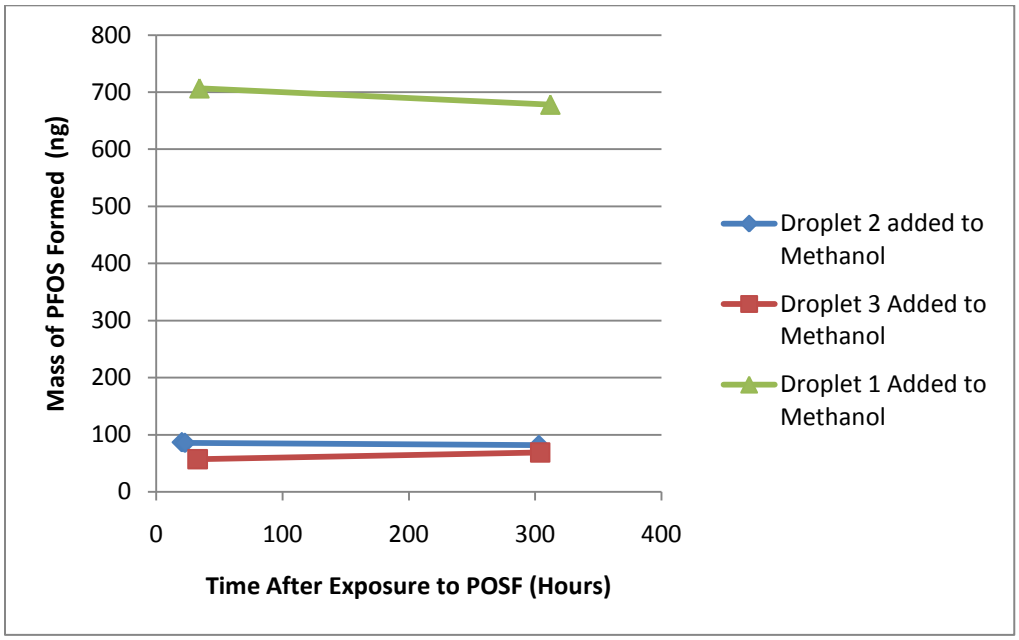

Figure 9 Change in PFOS Formed Over Time for Droplets Added to Methanol

Verification that protic solvents cause rapid hydrolyzation of POSF can be seen below in Table 5. Samples in the table were exposed to POSF and then placed into acetonitrile and analyzed. Twenty-four hours later the samples were analyzed again to determine how much PFOS was formed as water was scavenged inside the vial. Afterwards 100 µl of methanol was added to each sample, an increase in PFOS was observed in both containers. The values shown below are the PFOS concentrations immediately before and after the addition of methanol to the containers.

Table 5 Comparison of Sample Concentrations Prior to and After Addition of 100 µL of Methanol

Sample Info	ng/mL PFOS Present
1mL H20 in auto sampler vial †	11.70
1mL H20 in auto sampler vial, Methanol added †	14.40
1mL H20 in insert ‡	6.60
1mL H20 in insert Methanol added ‡	19.05

† Represents a sample where POSF was suspended above water. ‡ A sample where POSF was immersed in water and a sub-sample was withdrawn for analysis.

As can be seen above the presence of a protic solvent caused the concentration of PFOS in the samples to increase dramatically. The smaller increase observed in the first droplet is likely related to the rate at which POSF diffused from the suspended droplet to the water surface. Since the droplet was only exposed for 10 minutes it is possible only a small amount of POSF was able to diffuse to the water's surface. In the submerged sample the majority of POSF remained in the bottom of the container as a micelle like structure. The small amount of POSF present in the acetonitrile was slowly reacting with water placed in the acetonitrile.

In order to gain a better understanding of how fast POSF partitioned to the surface of the droplet from the headspace, droplets were exposed for varying time periods. Three one microliter droplets were exposed for time periods ranging from five minutes to 60 minutes. After exposure the droplets were placed in methanol to rapidly hydrolyze any unreacted POSF. Analysis of these experiments produced an unusual result in which droplets exposed for shorter time periods had higher concentrations than those exposed for longer times. Averaged values for time points from these experiments can be seen below in Figure 10. Standard error was calculated and is represented by error bars in the Figure 10.

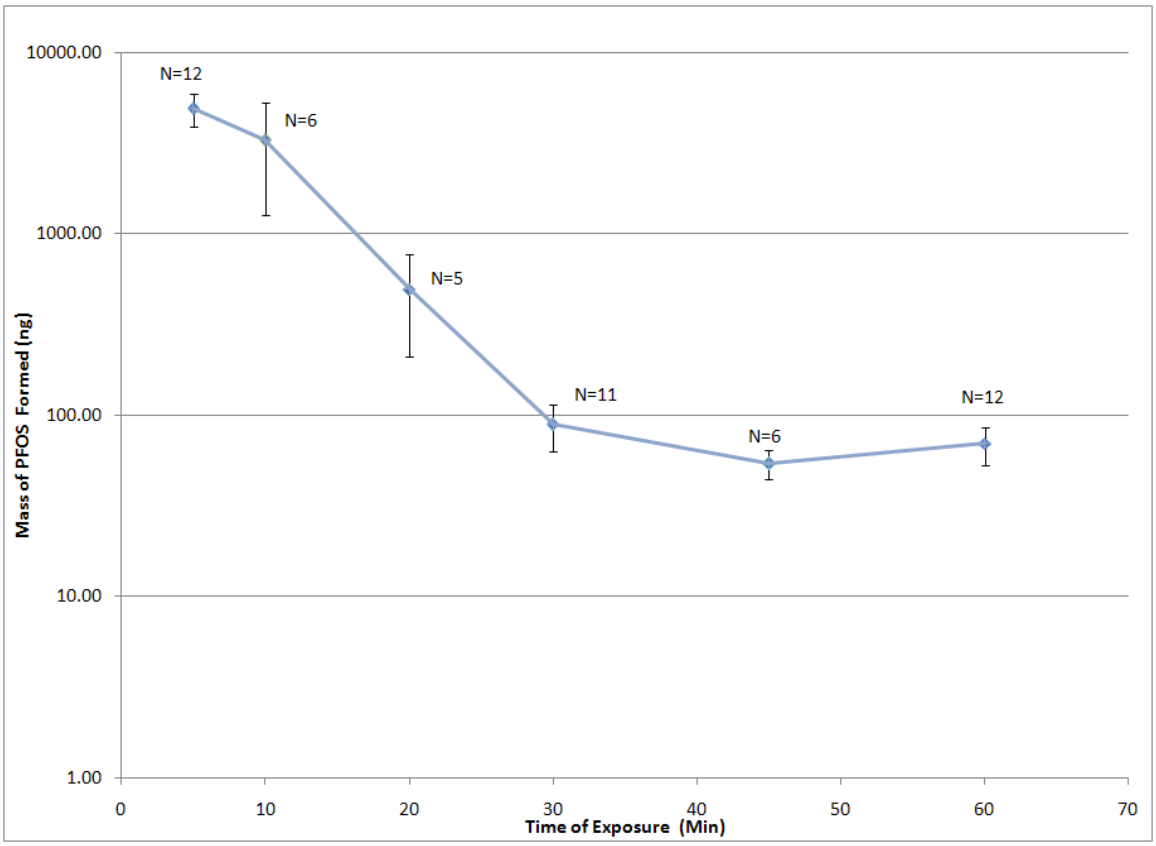

Figure 10 Average 1 µL Droplet Values, Comparing Time and PFOS Produced

As seen above in Figure 10, droplets exposed for five minutes were found to contain significantly more PFOS than those exposed for longer time periods however it is not completely understood as to why this phenomenon occurs. The use of methanol ensures that all unreacted POSF on the droplet would be reacted to form PFOS. Therefore it is unlikely the decrease in PFOS produced seen in Figure 10 would be the result of some samples having had more time to react in solution prior to analysis than others. A more reasonable explanation for the decrease in PFOS formed involves a decrease in reactive POSF on the droplets surface. This decrease may be caused by the formation of PFOS on the droplet, which in turn orients itself in such a way as to force

POSF from the droplet. An illustration depicting this removal of POSF can be seen below in Figure 11.

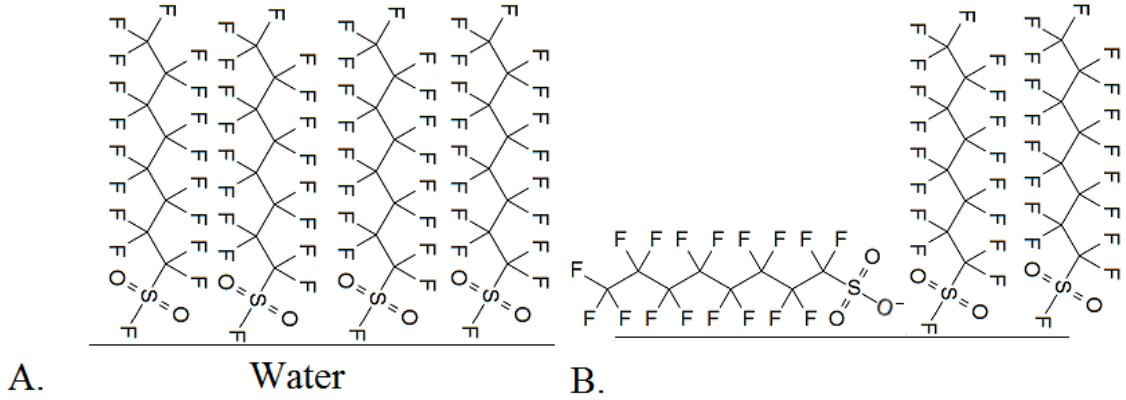

A. POSF on water droplet prior to PFOS formation. B. PFOS forms forcing unreacted POSF from the surface of the droplet.

Figure 11 Proposed Method of POSF Leaving Water Droplet

Another reason for the decrease in PFOS may be the hydrolysis of POSF to PFOS which also produces Hydrofluoric acid (HF). The dissociation of HF inside the suspended water droplet may result in a net charge forming on the droplet that expels POSF from the droplets surface. The formation and dissociation of Hydrofluoric acid may also result in a change in the water droplet's pH. According to Lehmler the hydrolysis of POSF to PFOS is base catalyzed reaction, therefore a decrease in pH may result in a slower formation of PFOS (Lehmler, 2005).

A change in the pH of the water droplet may play a role in the elimination of POSF from the droplets surface. PFOS is a strong acid and therefore is commonly measured in nature in its ionic form without the hydrogen on the sulfonic acid ($-SO_2H$) group. Therefore it is reasonable to assume that PFOS would dissociate after formation inside the water droplet. The dissociation of PFOS and HF could cause a significant

decrease in the pH of the aerosol droplet. This decrease in pH could result in expulsion of POSF from the surface of the aerosol droplet.

Another less plausible explanation is that PFOS leaves the droplet after it is formed. This is unlikely given the fact that PFOS is very water soluble, and non-volatile.

Conclusions:

This work has demonstrated that the volatile, PFOS- precursor POSF will react on the surface of suspended aerosol water droplets to form PFOS. The air-water interface present appears to aid this reaction as POSF exposed underwater formed far less PFOS. Through the use of non-reactive aprotic solvents it was possible to demonstrate the surface reaction of POSF is slower than the rate of diffusion into the suspended droplets. Finally, time variant experiments were useful in showing that the amount of PFOS formed is time dependent. Droplets exposed for more than 5 minutes produced less PFOS than droplets exposed for 60 minutes. Though the mechanism is not entirely understood it is believed that POSF is forced from the droplet resulting in less PFOS formed at longer time intervals.

Future Work:

Although this work demonstrates that PFOS can form on aerosol droplets, it also generates new questions to be addressed by future experiments. As discussed earlier it is unlikely that PFOS would leave the water droplet after formation, yet droplets exposed for longer time periods unexpectedly produce less PFOS. Future studies examining the loss of POSF from the droplets surface should be conducted to confirm or eliminate this theory as being responsible for reduced PFOS formation.

Possible experiments could include exposure of water droplets pre-concentrated with PFOS. Assuming PFOS formation forces POSF from the surface of droplets then the pre-concentrated droplets should produce less PFOS compared to pure water droplets. Similarly water doped with hydrofluoric acid could be exposed and compared to normal water droplets to determine if F^- ions are responsible for decreased PFOS production.

Additionally a strong acid could be added to water prior to droplet exposure in an attempt to alter the pH of the droplet. A comparison in the amount of PFOS produced could then be made between the lower pH water and unaltered water to determine if pH plays a role in PFOS production.

Although it was not possible to determine the rate of hydrolysis using the methods described earlier use of isotopically labeled solvents would make this possible. If ^{18}O labeled water were exposed to volatilized POSF and later placed in methanol a comparison could be made between the PFOS produced. Heavier PFOS would be hydrolyzed on the droplets surface, and PFOS with the normal mass of 499 would have been hydrolyzed in methanol.

References

3 M Company. (1999). Fluorochemical Use, Distribution, and Release Overview.

3M Company. (2001). *Hydrolysis Reactions of Perflurooctane Sulfonate (PFOS).* St Paul : 3M Environmental Labratory .

3M Company. (2001). *Screening Studies on the aqueous photolytic degradation of Potassium Perfluorooctane Sulfonate (PFOS).* St. Paul: 3M Environmental Lab.

3M Company. (2003). *Sulfonated Perfluorochemicals in the Environment: Sources, Dispersion, Fate and Effects.* EPA.

3M Corporation. (2000). 3M Phase Out Plan for POSF-Based Products.

3M Corporation. (1999). *The Science of Organic Fluorochemistry.* EPA Docket # OPPT -2002-0043-0006.

3M Corporation. (1999, Feburary 5). The Science of Organic Fluorochemistry. 1-12. St. Paul , Minnesota.

Ahrens, L., Barber, J. L., Xie, Z., & Ebinghaus, R. (2009). Longitudinal and Latiudinal Distribution of Perflouoroalkyl Compounds in the Surface Water of the Atlantic Ocean. *43* (9), 3122-3127.

Ahrens, L., Siebert, U., & Ebinghaus, R. (2009). Temporal Trends of Polyfluoroalkyl Compounds in Harbor Seals (Phoca vitulina) from the German Bight, 1999-2008. *Chemosphere* (76), 151-158.

Apelberg, B. J., Witter, F. R., Herbstman, J. B., Calafat, A. M., Halden, R. U., Needham, L. L., (2007). Cord Serum Concentrations of Perfluorooctane Sulfonate (PFOS) and Perfluorooctanoate (PFOA) in Relation to Weight and Size at Birth. *115* (11), 1670-1676.

Armitage, J. M., Schenker, U., Scheringer, M., Martin, J. W., Macleod, M., & Cousins, I. T. (2009). Modeling the Global Fate and Transport of Perfluoroctane Sulfonate (PFOS) and Precursor Compounds in Relation to Temporal Trends in Wildlife Exposure. *43* (24), 9274-9280.

Beach, S. A., Newsted, J. L., Coady, K., & Giesy, J. P. (2006). *Ecotoxicological Evaluation of Perfluoroctanesulfonate (PFOS).* Rev Environmental Contaminats Toxicology.

Bossi, R., Riget, F. F., & Dietz, R. (2005). Temporal and Spatial Trends of Perfluorinated Compounds in Ringed Seal (Phoca hispida) from Greenland. *Environmental Science & Technology , 39* (19), 7416-7422.

Butt, C. M., Muir, D. C., Stirling, I., Kwan, M., & Mabury, S. A. (2007). Rapid Response of Arctic Ringed Seals to Changes in Perfluoroalkyl Prodcution. *Environmental Science & Technology , 41* (1), 42-49.

Dallaire, R., Ayotte, P., Pereg, D., Déry, S., Dumas, P., Langlois, E., (2009). Determinants of Plasma Concentrations of Perfluorooctanesulfonate and Brominated Organic Compounds in Nunavik Inuit Adults (Candada). *Environmental Science & Technology , 43* (13), 5130-5136.

D'Eon, J. C., Hurley, M. D., Wallington, J. T., & Mabury, S. A. (2006). Atmospheric Chemistry of N-methyl Perfluorobutane Sulfonamidoethanol, C4F9SO2N(CH3)CH2CH2OH: Kinetics and Mechanism of Reaction with OH. *Environmental Science & Technology , 40* (6), 1962-1968.

Dietz, R., Bossi, R., Sonne, C., & Born, W. (2008). Increasing Perfluoroalkyl Contaminants in East Greenland Polar Bears (Ursus maritimus): A New Toxic Threat to the Arctic Bears. *Environmental Science & Technology , 42* (7), 2701-2707.

Ehresman, D. J., Froehlich, J. W., Olsen, G. W., Chang, S.-C., & Butenhoff, J. L. (2007). Comparison of Human Whole Blood, Plasma, and Serum Matrices for the Determination of Perfluorooctanesulfonate (PFOS), Perfluorooctanoate (PFOA) and Other Fluorochemicals. *103*, 176-184.

Ellefson. (2002 A). *Solubility in Water, Natural Seawater, an Aqueous Solution of 3.5% Sodium Chloride, and N-Octanol with Subsequent Calculation of the N-Octanol:Water Partion Coffecient (Kow)of PFOS for each of the Aqueous Matrices.* EPA.

Ellefson, M. E. (2001). *Solubility of Perfluoro-1-octanesulfonyl Fluoride (POSF) in Water.*

Ellefson, M. E. (2001). *Solubility of Perfluoro-1-octanesulfonyl Fluoride (POSF) in Water.* St. Paul: 3M Enviironmental Laboratory.

EPA. (2002). *EPA-HQ-OPPT-2002-0051-0027.* EPA .

EPA. *EPA-HQ-OPPT-2003-0012-0006.*

EPA/OPPT/Exposure Assessment Tools and Models/Estimation Program Interface (EPI) Suite Version 3.12 (August 17, 2004). Computer software. *US Environmental Protection Agency*. Vers. 4.00. Web. 10 May 2010. <http://www.epa.gov/oppt/exposure/pubs/episuite.htm>

Giesy, J. P., & Kannan, K. (2001). Global Distribution of Perfluorooctane Sulfonate in Wildlife. (35), 1339-1342.

Giesy, J. P., & Kannan, K. (2002). Perfulorochemical Surfactants in the Environment. *Envrionmental Science & Technology* , 146A-151A.

Hart, K., Gill, V. A., & Kannan, K. (2009). Temporal Trends (1992-2007 of Perfluorinated Chemicals in Northern Sea Otters (Enhydra lutris kenyoni) from South-Central Alaska. *Archives of Environmental Contamination and Toxicology , 56*, 607-614.

Haug, L. S., Thomsen, C., & Becher, G. (2009). Time Trends and the Influence of Age and Gender on Serum Concentrations of Perfluorinated Compounds in Archived Human Samples. (43), 2131-2136.

Holmstrom, K. E., Jarnberg, U., & Bigner, A. (2005). Temporal Trends of PFOS and PFOA in Guillemot Eggs from the Baltic Sea, 1968-2003. *Environmental Science & Technology* (39), 80-84.

Hu, W. y., Jones, P. D., DeCoen, W., King, L., Fraker, P., Newsted, J., (2003). Alterations in Cell Membrane Properties caused by Perfluorinated Compounds. *135*, 77-88.

Hu, W., Jones, P. D., Upham, B. L., Trosko, J. E., Lau, C., & Giesy, J. P. (2002). Inhibition of Gap Junction Intercellular Communication by Perfluorinated Compounds in Rat Liver and Dolphin Kidney Epithelial Cell Lines in Vitro and Sprague-Dawley Rats in Vivo. (68), 429-236.

Kannan, K., Koistinen, J., Beckmen, K., Evans, T., Gorzelany, J. F., Hansen, K. J., (2001). Accumulation of Perfluorooctane Sulfonate in Marine Mammals. *Envrionmental Science & Technology* (35), 1593-1598.

Kelly, B. C., Ikonomou, M. G., Blair, J. D., Surridge, B., Hoover, D., Grace, R., (2009). Perfluoroalkyl Contaiminats in an Arctic Marine Food Web: Trophic Magnification and Wildlife Exposure. *Environmental Science Technology , 43* (11), 4037-4043.

Lau, C., Butenhoff, J. L., & Rogers, J. M. (2004). The Developmental Toxicology of Perfluoroalkyl Acids and their Derivatives. *Toxicology and Applied Pharamcology* , 231-241.

Lehmler, H. J. (2005). Synthesis of Environmentally Relevent Fluorinated Surfactants -- A Review. *Chemosphere* (58), 1471-1496.

Lowen, M., Wania, F., Wang, F., & Tomy, G. (2008). Altitudinal Transect of Atmospheric and Aqueous Fluorinated Organic Compounds in Western Canada. *Environtal Science & Technology , 42* (7), 2374-2379.

Martin, J. W., Muir, D. C., Moody, C. A., Ellis, D. A., Kwan, W. C., Solomon, K. R., (2002). Collection of Airborne Fluorinated Organics and Analysis by Gas Chromotography/Chemical Ionization Mass Spectrometry. *Analatical Chemistry , 74* (3), 584-490.

McMurdo, C. J., Ellis, D. A., Webster, E., Butler, J., Christensen, R. D., & Reid, L. K. (2008). Aerosol Enrichment of the Surfactant PFO and Mediation of the Water-Air Transport of Gaseous PFOA. *Environmental Science & Technology , 42* (11), 3969-3974.

Moody, C. A., & Field, J. A. (2000). Perfluorinated Surfactants and the Environmental Implications of Their Use in Fire-Fighting Foams. *Environmental Science & Technololgy , 34* (18), 3864-3870.

Moody, C. A., Martin, J. A., Kwan, W. C., Muir, D. C., & Mabury, S. A. (2002). Monitoring Perfluorinated Surfactants in Biota and Surface Water Samples Following An Accidental Release of Fire-Fighting Foam into Etobicoke Creek. *Enivornmental Science & Technology , 36* (4), 545-551.

OECD. (2002). Hazard Assessment of Perfluorooctane Sulfonate (PFOS) and its Salts. *17*.

Olsen, G. W., Burris, J. M., Burlew, M. M., & Nandel, J. H. (2003). Epidemiologic Assesment of Worker Serum Perfluoroctanesulfonate (PFOS) and Perfluoroctanoate (PFOA) Concentrations and Medical Surveillance Examinations. *45* (3), 260-270.

Paul, A. G., Jones, K. C., & Sweetman, A. J. (2009). A First Global Production Emission, and Environmental Inventory for Perfluorooctane Sulfonate. *Environmental Science & Technology , 43* (2), 386-392.

Plumlee, M. H., McNeill, K., & Reinhard, M. (2009). Indirect Photolysis of Perfluorochemicals: Hydroxyl Radical-Initiated Oxidation of N-Ethyl Perfluorooctane

Sulfonamido Acetate (N-EtFOSAA) and other Perfluoroalkanesulfonamides). *Environmental Science & Technology , 43* (10), 3662-3668.

Seacat, A. M., Thomford, P. J., Hansen, K. J., Olesen, G. W., Case, M. T., & Butenhoff, J. L. (2002). Subchronic Toxicity Studies on Perfluoroctanesulfonate Potassium Salt in Cynomolgus Monkeys. *Toxicological Sciences* , 249-264.

Shciavone, A., Corsolini, S., Kannan, K., Tao, L., Trivelpiece, W., Torres, D., (2009). Perfluorinated contaminants in fur seal pups and penguin eggs from South Shetland, Antarctica. *Science of the Total Environment* (407), 3899-3904.

Simcik, M. F. (2005). Global transport and fate of perfluorochemicals. (7), 759-763.

Simcik, M. F., & Dorweiler, K. J. (2006). Ratio of Perfluorchemical Concentrations as a Tracer of Atmosphereic Deposition to Surface Waters. *39* (22), 8678-8693.

Smithwick, M., Mabury, S. A., Solomon, K. R., Sonne, C., Martin, J. W., Born, E. W., (2005). Circumpolar Study of Perfluoroalkyl Contaminants in Polar Bears (Ursus maritimus). *Environmental Science & Technology , 39* (15), 5517-5523.

Smithwick, M., Norstrom, R. J., Mabury, S. A., Solomon, K., Evans, T. J., Stirling, I., (2006). Temporal Trends of Perfluoroalkyl Contaminatnts in Polar Bears (Ursus maritimus) from Two Locations in the North American Arctic, 1972-2002. *Environmental Science & Technology , 40* (4), 1139-1143.

So, M. K., Yamashita, N., Taniyasu, S., Jiang, Q., Giesy, J. P., Chen, K., (2006). Health Risks in Infants Associated with Exposure to Perfluorinated Compounds in Human Breast Milk from Zhoushan, China. *Environmental Science & Technology , 40* (9), 2924-2929.

Stock, N. L., Lau, F. K., Ellis, D. A., Martian, J. W., Muir, D. C., & Mabury, S. A. (2004). Polyfluorinated Telomer Alcohols and Sulfonamides in the North American Troposphere. *38* (4), 991-996.

STS Conslutants, Ltd. (2007). *Surface Water Quality Criterion for Perfluorooctane Sulfonic Acid.* Minnesota Pollution Control Agency.

Taves, D. R. (1968). Evidence that there are Two Froms of Fluoride in Human Serum. *217*, 1050-1051.

Tomy, G. T., Budakowski, W., Halldorson, T., Helm, P. A., Stern, G. A., Friesen, K., (2004). Fluorinated Ogranic Compounds in an Eastern Arctic Marine Food Web. *Environmental Science & Technology , 38* (24), 6475-6481.

USEPA. (1996). *OPPTS 830.7550 Partition Coefficient (n-Octanol/Water), Shake Flask Method.* EPA, Office of Prevention, Pesticides and Toxic Substances .

Vanden Heuvel, J. P., Thompson, J. T., Frame, S. R., & Gillies, P. J. Differential Activation of Nuclear Receptors by Perfluorinated Fatty Acid Ananalogs and Natural Fatty Acids. A Comparison of Human, Mouse, and Rat Peroxisome Peroliferator-Activated Receptor-a, -B and -y, Liver X Receptor -B and Retinoid X Receptor -a. (2006) *Toxicological Sciences 92* (2), 476-489.

Verreault, J., Berger, U., & Gabrielesen, G. W. (2007). Trends of Perfluorinated Alkyl Substances in Herring Gull Eggs from Two Costal Colonies in Northern Norway: 1983-2003. *Environmental Science & Technology , 41* (19), 6671-6677.

Yamashita, N., Kannan, K., Horii, Y., Okazawa, T., Petrick, G., & Gamo, T. (2004). Analysis of Perfluorinated Acids at Parts-Per-Quadrillion Levels in Seawater Using Liquid Chromatography-Tandem Mass Spectrometry. *Environmental Science & Technology , 38* (21), 5522-5528.

Appendix A: Perfluorochemical Names and Structures.

Perfluorooctanesulfonic Acid – PFOS

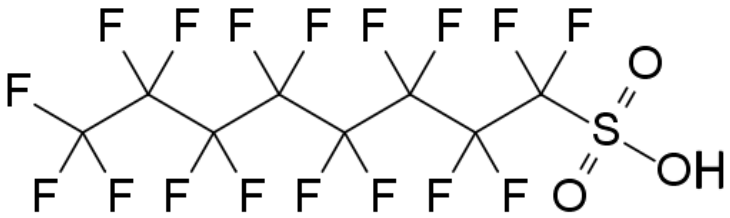

Perfluoroctanesulfonyl Fluoride – POSF

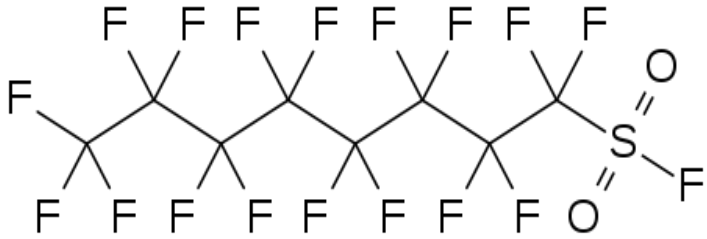

Perfluoroctanoaic Acid -- PFOA

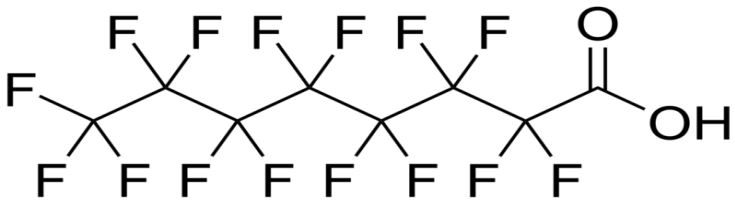

Perfluorooctanoate -- (PFO)

Appendix B. Diagram of Experimental Setup.

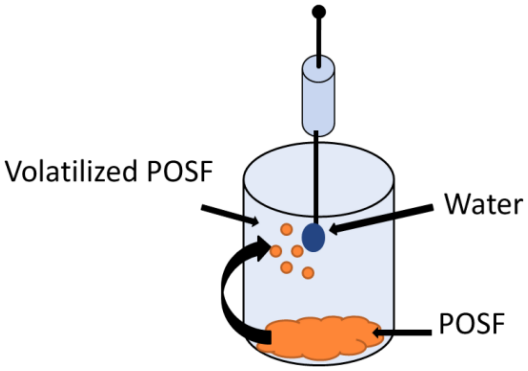

Example of vial and syringe setup during normal water droplet suspension experiments.

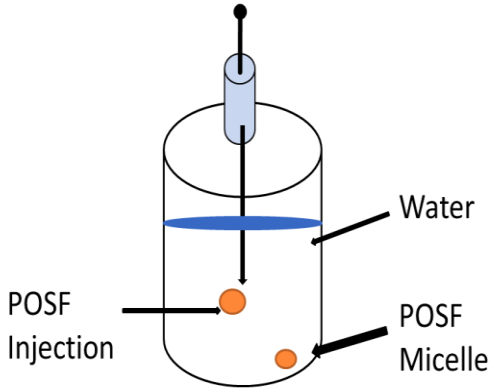

Example of underwater POSF exposure.

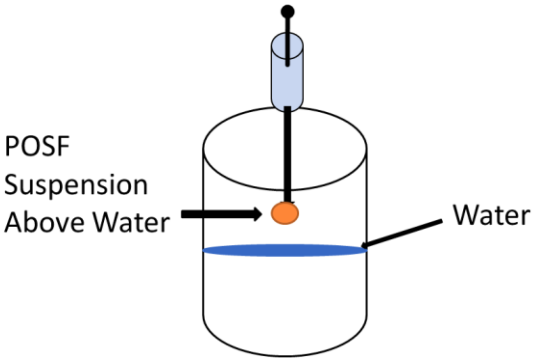

Example of vial and syringe setup during POSF droplet suspension experiments.

Appendix C. Experimental Data.

POSF Exposed Underwater Raw Data.

File Name	Sample Info	Peak Area	Actual PFOS in Standard (ng)	PFOS Present Using Calibration Curve (ng)	Average (ng)
09072302.D	5 ng	69515.1	5	5.85	
09072303.D	25 ng	265630.6	25	20.04	
09072304.D	50 ng	711902.5	50	52.32	
09072305.D	100 ng	1411684.8	100	102.94	
09072306.D	250 ng	3428422	250	248.83	
09072330.D	1mL H20 2 uL POSF	11642.9		1.67	
09072335.D	1mL H20 2 uL POSF	15616		1.95	
09072339.D	1mL H20 2 uL POSF	12637.5		1.74	1.79
09072343.D	1 mL H20 1 uL POSF	12979.7		1.76	
09072347.D	1 mL H20 1 uL POSF	14315		1.86	
09072351.D	1 mL H20 1 uL POSF	1647.3		0.94	1.52
09072355.D	2 mL H20 1 uL POSF	19985.4		2.27	
09072359.D	2 mL H20 1 uL POSF	20577.5		2.31	
09072363.D	2 mL H20 1 uL POSF	15855.5		1.97	2.19
09072369.D	2 mL H20 2 uL POSF	30371.3		3.02	
09072371.D	2 mL H20 2 uL POSF	17639.4		2.10	
09072375.D	2 mL H20 2 uL POSF	9654.6		1.52	2.22
Calibration Curve Equation	Y=13824x-11406				

Bulk interface: Suspended POSF droplet exposed above one milliliter container of water.

File Name	Sample Info	Peak Area	Surface Area ($mm^{2)}$	499 Peak Area	503 Peak Area	PFOS Present Using Calibration Curve (ng)
09072834.D	5 ng	53230.50		53231	9313.1	2.40
09072838.D	25 ng	231459.50		231460	10757.4	26.16
09072842.D	50 ng	434420.80		434421	11829.8	53.21
09072846.D	100 ng	772197.40		772197	17541.1	98.24
09072850.D	250 ng	1712427.60		1712428	1854.2	223.57
09072854.D	POSF Over Water #1	46787.60	71.63	46788	10064.4	1.54
09072858.D	POSF Over Water #2	46457.80	71.63	46458	3280.3	1.50
09072862.D	POSF Over Water #3	58441.00	71.63	58441	14761.4	3.09
09072866.D	Water Droplet #1	7437028.00	4.84	7437028	4140	986.65
09072870.D	Water Droplet #2	1323585.10	4.84	1323585	--	171.74
09072874.D	Water Droplet #3	2457592.50	4.84	2457593	--	322.90
09072878.D	Air Blank #1	18181.70	4.84	18182	--	-2.27
09072882.D	Air Blank #2	7424.20	4.84	7424	--	-3.71
09072886.D	Air Blank #3	10182.50	4.84	10183	--	-3.34
Calibration Curve Equation	y = 7501.9x + 35242					

Addition of Methanol to POSF samples that were placed in acetonitrile.

File Name	Sample Info	Actual PFOS in Standard (ng)	499 Peak Area	503 Peak Area	PFOS Present Using Calibration Curve (ng)
09072834.	5 ng	5.00	53230.50	9313.10	2.40
09072838.	25 ng	25.00	231459.50	10757.40	26.16
09072842.	50 ng	50.00	434420.80	11829.80	53.21
09072846.	100 ng	100.00	772197.40	17541.10	98.24
09072850.	250 ng		1712427.60	1854.20	223.57
09072812.	1mL H20 in auto sampler vial		91323.90	6821.40	7.48
09072816.	1mL H20 in insert		53059.80	7840.40	2.38
09072823.	1mL H20 in auto sampler vial w/ C^{13} added		111585.10	21464.00	10.18
09072827.	1mL H20 in insert w/ C^{13} added		146512.10	9903.60	14.83
Calibration Curve Equation	Calibration Curve Equation	y = 7501.9x + 35242			

One microliter suspended water droplets placed in acetonitrile.

File Name	Sample Info	499 Peak Area	PFOS Present Using Calibration Curve (ng)
91105021.D	5 ng	106220.40	3.71
91105025.D	25 ng	623318.90	23.60
91106020.D	50 ng	1342141.80	51.24
91106024.D	100 ng	2569295.50	98.44
91106028.D	250 ng	5438757.50	208.80
09110505.D	2nd Drop 11/5/09	133805.10	4.77
09110510.D	2nd Drop 11/5/09	271241.60	10.05
09110516.D	2nd Drop 11/5/09	849760.30	32.30
91105005.D	2nd Drop 11/5/09	1094825.00	41.73
91105009.D	3rd Drop 11/5/09	1398677.40	53.42
91105013.D	1st Drop 11/5/09	1446362.30	55.25
9110517.D	Air Blank	4571.70	-0.20
91105021.D	5 ng	106220.40	3.71
91105025.D	25 ng	623318.90	23.60
91106032.D	Blank Acet	2207.00	-0.29
91106036.D	Needle 1 Acet	13730.40	0.15
91106040.D	Needle 2 Acet	4841.00	-0.19
91106045.D	Needle 3 Acet	10762.90	0.04
91106066.D	2nd Drop Rerun	5347146.50	205.27
91106070.D	3rd Drop Rerun	5212728.50	200.10
91106074.D	1st Drop Rerun	5395253.50	207.12
91106078.D	Air Blank Rerun	5059.90	-0.18
91106085.D	5 ng	382675.50	14.34
91106086.D	25 ng	698975.20	26.51
91106094.D	25 ng	419576.70	15.76
91106098.D	50 ng	846073.50	32.16
91106102.D	3rd Drop Rerun	5289699.50	203.06
91106106.D	1st Drop Rerun	4848487.00	186.10
91106133.D	2nd Drop Rerun	5455420.50	209.44
Calibration Curve Equation	y = 26001x - 9816.2		

One microliter suspended water droplets placed in acetonitrile.

File Name	Sample Info	499 Peak Area	PFOS Present Using Calibration Curve (ng)
09082704.D	Water Droplet #1	232576.50	26.30403388
09082708.D	Water Droplet #2	2719888.80	429.9050432
09082712.D	Water Droplet #3	309703.90	38.81902707
09082724.D	5 ng	58914.80	-1.874991887
09082728.D	25 ng	300805.00	37.37505679
09082732.D	50 ng	344715.10	44.50008113
09082736.D	100 ng	65354.00	-0.830142143
09082740.D	250 ng	1555838.00	241.0216136
Calibration Curve Equation	y = 6162.8x + 70470		

One microliter suspended water droplets placed in acetonitrile.

File Name	Sample Info	499 Peak Area	PFOS Present Using Calibration Curve (ng)
09082709.D	Water Droplet #1	729258.30	49.91691668
09082713.D	Water Droplet #2	4105740.80	280.1420974
09082717.D	Water Droplet #3	1190148.10	81.34264967
09082721.D	Air Blank	17755.5	1.403156962
09082724.D	5 ng	76321.50	5.39647484
09082728.D	25 ng	3916141.20	267.2142643
09082732.D	50 ng	344715.10	23.69687031
09082736.D	100 ng	1968625.20	134.4230465
09082740.D	250 ng	3538767.80	241.4830901
9090844.D	Needle 1Acet.	60816.8	4.339288149
9090848.D	Neelde 1 H20	12159	1.021560071
9090852.D	Needle 2 Acet.	320549.8	22.04916133
90900856.D	Neelde 2 H20	10238.1	0.890583663
9090860.D	Old Needle Acet.	2119	0.336983499
9090864.D	Old Neelde H20	9868.3	0.86536888
09090872.D	Water Droplet #1 Rerun	3467516.8	236.6248466
09090876.D	Water Droplet #2 Rerun	9932134	677.414237
09090880.D	Water Droplet #3 Rerun	2947750.50	201.1846243
Calibration Curve Equation	y = 14666x-2823.2		

One microliter suspended water droplets placed in acetonitrile.

File Name	Sample Info	499 Peak Area	PFOS Present Using Calibration Curve (ng)
90923004.D	Water Droplet #1	26426.20	0.81180323
90923008.D	Water Droplet #2	69608.80	4.025511647
90923012.D	Water Droplet #3	263599.30	18.46255116
90923016.D	Air Blank	3044.1	-0.928324775
90923020.D	5 ng	72694.40	4.255146238
90923024.D	25 ng * value from later used here	283850.00	19.96963608
90923028.D	50 ng	713100.90	51.91507777
90923032.D	100 ng	1442649.60	106.2090943
90923036.D	250 ng	3343212.80	247.6516187
90923040.D	Water Droplet #1 Rerun	122910.8	7.992319714
90923044.D	Water Droplet #2 Rerun	193482.4	13.24435514
9092348.D	Water Droplet #3 Rerun	497422.10	35.86396517
9092353.D	Air Blank Acet.	--	--
90923057.D	Needle 1Acet.	3714.1	-0.878462454
90923061.D	Needle 2 Acet.	1916.5	-1.012242316
90923065.D	Needle 3 Acet.	--	--
90923066.D	25 Ng Standard *	283850	19.96963608
90923070.D	50 Ng Standard	743825.4	54.20163727
90923072.D	Water Droplet #1 Rerun	159690.5	10.72951552
90923076.D	Water Droplet #2 Rerun	248013	17.30259731
90923080.D	Water Droplet #3 Rerun	666028.60	48.41189254
09092405.D	1st Drop Rerun	389015.9	27.79622684
09092409.D	25 ng Sample	277815.7	19.52055518
09092413.D	50 ng Sample	733669.1	53.44579147
09092417.D	2nd Drop Rerun	723783.70	52.71010642
09092421.D	3rd Drop Rerun	1159174.6	85.11249535
09092425.D	Air Blank Rerun	4407.9	-0.826828905
09092405.D	1st Drop Rerun	395430.8	28.27363251
09092405.D	2nd Drop Rerun	618784.1	44.89589194
09092405.D	50 ng Standard	768453.8	56.03451663
09092405.D	3rd Drop Rerun	1120727	82.25117214
Calibration Curve Equation	y = 13437x + 15518		

One microliter suspended water droplets placed in acetonitrile.

File Name	Sample Info	499 Peak Area	PFOS Present Using Calibration Curve (ng)
90925005.D	Water Droplet #2	247904.20	13.48665366
90925009.D	Water Droplet #3	400353.70	21.98202842
90925013.D	Water Droplet #1	658633.30	36.37487322
90925016.D	Air Blank	3044.1	-0.158378378
90925021.D	5 ng	137437.00	7.330777375
90925025.D	25 ng	346256.10	18.96739482
90925029.D	50 ng	934234.20	51.73296183
90925033.D	100 ng	5333360.00	296.8778936
90925037.D	250 ng	731198.40	40.41862357
90925041.D	Blank Needle Acet.	11465	0.310883254
90925045.D	Needle 1Acet.	11465	0.310883254
90925049.D	Needle 2 Acet.	4479.6	-0.078383951
90925053.D	Needle 3 Acet.	5540.6	-0.019258846
90925064.D	25 Ng Standard	301510.3	16.47389802
90925068.D	50 Ng Standard	991502	54.92425745
90925060.D	Water Droplet #2 Rerun	872959.9	48.31840067
90925072.D	Water Droplet #3 Rerun	983178.1	54.46040123
90925076.D	Water Droplet #1 Rerun	597937.90	32.99257175
Calibration Curve Equation	y = 17945x - 5886.2		

One microliter suspended water droplets placed in acetonitrile.

File Name	Sample Info	499 Peak Area	PFOS Present Using Calibration Curve (ng)
09072866.D	Water Droplet #1	7437028.00	990.8804436
09072870.D	Water Droplet #2	1323585.10	175.9611698
09072874.D	Water Droplet #3	2457592.50	327.123862
09072878.D	Air Blank #1	18181.70	1.951465629
09072882.D	Air Blank #2	7424.20	0.517495568
09072886.D	Air Blank #3	10182.50	0.885175755
Cal Std			
09072834.D	5 ng	53230.50	6.623455391
09072838.D	25 ng	231459.50	30.3813034
09072842.D	50 ng	434420.80	57.43595622
09072846.D	100 ng	772197.40	102.4614298
09072850.D	250 ng	1712427.60	
Calibration Curve Equation	y = 7501.9x + 35242		

One microliter suspended water droplets placed in acetonitrile.

File Name	Sample Info	499 Peak Area	PFOS Present Using Calibration Curve (ng)
09100505.D	Water Droplet #2 (9/25/09)	1107835.20	71.89447368
0910059.D	Water Droplet #3 (9/25/09)	3131074.7	212.0080125
09100513.D	Water Droplet #1 (9/25/09)	2299079.5	154.3906163
09100517.D	Old Water Droplet #1 (9/23/09)	486814.8	28.88752078
09100521.D	25 ng Standard	442748.00	25.83580332
09100525.D	50 ng Standard	798549.90	50.4758241
09100534.D	Old Water Droplet #2 (9/23/09)	163797.90	6.517929363
09100538.D	Old Water Droplet #3 (9/23/09)	1088560.4	70.55965374
09100542.D	5 ng	106733.9	2.566128809
09100546.D	25 ng	440177.00	25.65775623
09100550.D	50 ng	774715.60	48.82524931
09100554.D	100 ng	1579527.10	104.5601177
09100558.D	250 ng	3656590.50	248.4010734
Calibration Curve Equation	y = 14440x + 69679		

One microliter suspended water droplets exposed for varying time periods (in methanol).

File Name	Description	Area of 499 Peak	Corrected Area of 499 Peak	Area of 503 Peak	RRF	Mass of PFOS Observed (ng)
1002107.D	Blank	36632.4				
1002108.D	Calibration Std	103881.1	91462.91	108316.1	1.01	51.34
1002119.D	Blank					
1002120.D	5 Min 2	5509748.5	5497330.31	43709.4		3823.24
1002121.D	Blank	47646.4				
1002122.D	5 Min 3	3678899	3666480.81	52567		2120.27
1002123.D	Blank	39576.1				
1002124.D	5 Min 1	1793319.4	1780901.21	44796.3		1208.52
1002125.D	Blank	36656.6				
1002126.D	Blank	48273.1	35854.91			
1002129.D	Blank	68115.8				
1002130.D	Blank	75567.5				
1002132.D	Calibration Std	43866	31447.81	40821.1	0.92	42.73
1002133.D	Blank	14183.9				
1002134.D	10 Min 2	63983.7	51565.51	25285.4		61.99
1002135.D	Blank	14123				
1002136.D	10 Min 3	34496.4	22078.21	2859.1		234.74
1002137.D	Blank	14074.4				
1002138.D	10 Min 1	18501.9	6083.71	29466.4		6.28
1002141.D	Blank	11805.6				
1002142.D	20 Min 2	56046	43627.81	27283.1		48.61
1002143.D	Blank	13397				
1002144.D	20 Min 3	39543.8	27125.61	21411.9		38.51
1002145.D	Blank	13996.9				
1002146.D	20 Min 1	45885.8	33467.61	26134.8		38.93
1002147.D	Blank	13186.6				
1002149.D	Blank	13662.9				
1002150.D	Calibration Std	36954.4	24536.21	36065.7		20.68
1002151.D	Blank					
1002153.D	Blank	12046.5				
1002155.D	Blank	12640				
1002156.D	30 Min 2 (skip)		-12418.19			
1002157.D	Blank	14950				
1002158.D	30 Min 3	33967.6	21549.41	28910.2		22.66

One microliter suspended water droplets exposed for varying time periods (continued from above).

File Name	Description	Area of 499 Peak	Corrected Area of 499 Peak	Area of 503 Peak	RRF	Mass of PFOS Observed (ng)
10012401.D	45 Min 2	63379.9	50961.71	22090.6		70.13
10012402.D	Blank	15898				
10012403.D	45 Min 3	44887.7	32469.51	32590.9		30.29
10012404.D	Blank	13592.2				
10012405.D	45 Min 1	33750.8	21332.61	18515.6		35.02
10012406.D	Blank	16309.7				
10012408.D	Blank	13483.5				
10012409.D	Calibration Std	48314.8	35896.61	50600.8	0.85	36.23
10012410.D	Blank	14558.4				
10012411.D	60 Min 2	28382.1	15963.91	17555.1		27.64
10012412.D	Blank	12754.5				
10012413.D	60 Min 3	28095.9	15677.71	12843.4		37.11
10012414.D	Blank	14892.2				
10012415.D	60 Min 1	26414.9	13996.71	10978.1		38.76
10012418.D	Blank	11501.2				
10012419.D	Calibration Std	25030	12611.81	23140.6	0.65	21.39
10012420.D	Blank	11720.1				
Blank Average	12418.1875					

One microliter suspended water droplets exposed for varying time periods. (in Methanol)

File Name	Description	Area of 499 Peak	Corrected Area of 499 Peak	Area of 503 Peak	RRF	Mass of PFOS Observed (ng)
10042002.D	Blank	0				
10042003.D	Calibration Standard	5084.9	5084.9	6685.4	1.10	50.00
10042004.D	Blank	0				
10042005.D	5 Min Sample 2	370190.4	370190.4	2419.6		10057.65
10042006.D	Blank	0				
10042007.D	5 Min Sample 3	470289.7	470289.7	3018.4		10242.45
10042008.D	Blank	0				
10042009.D	5 Min Sample 1	625437.4	625437.4	4143		9923.93
10042010.D	Blank	0				
10042011.D	5 Min Blank	756.3	756.3	4096.7		12.14
10042012.D	Blank	0				
10042013.D	10 Min Sample 2	734563.7	734563.7	5004.4		9649.22
10042014.D	Blank	0				
10042015.D	10 Min Sample 3	836945.7	836945.7	5586.6		9848.38
10042016.D	Blank	0				
10042017.D	10 Min Sample 1	2913.6	2913.6	4737.1		40.43
10042018.D	Blank	0				
10042019.D	10 Min Air Blank	1814	1814	4894.60		24.36
10042020.D	Blank	0				
10042021.D	20 Min Sample 2	86656.3	86656.3	4109.80		1386.10
10042022.D	Blank	0				
10042023.D	20 Min Sample 1	50899.6	50899.6	3320.90		1007.57
10042024.D	Blank	0				
10042025.D	20 Min Air Blank	1132.4	1132.4	4644.80		16.03
10042026.D	Blank	0				
10042027.D	30 Min Sample 2	4127.4	4127.4	3643.00		74.48
10042028.D	Blank	0				
10042029.D	30 Min Sample 3	6173.4	6173.4	5281.20		76.84
10042030.D	Blank	0				

One microliter suspended water droplets exposed for varying time periods (continued from above).

File Name	Description	Area of 499 Peak	Corrected Area of 499 Peak	Area of 503 Peak	RRF	Mass of PFOS Observed (ng)
10042031.D	30m Min Sample 1	7673.3	7673.3	4977.3		0.00
10042032.D	Blank	0				
10042033.D	30 Min Air Blank	1244	1244	4595.20		0.00
10042034.D	Blank	0				
10042035.D	25 Ng Cal Std	2161	2161			
10042036.D	Blank	0				
10042037.D	Calibration Standard	6710.6	6710.6	9605.40	1.19	0.00
10042038.D	Blank	0				
10042039.D	45 Min Sample 2	9558.5	9558.5	6187.00		0.00
10042040.D	Blank	0				
10042041.D	45 Min Sample 3	4264.2	4264.2	4428.70		0.00
10042042.D	Blank	0				
10042043.D	45 Min Sample 1	4687.80	4687.80	4459.70		51.87
10042044.D	Blank	#REF!				
10042045.D	45 Min Air Blank	1180.70	1180.70			--
10042046.D	Blank	0.00				
10042047.D	60 Min Sample 2	8090.50	8090.50	4691.60		101.21
10042048.D	Blank	0.00				
10042049.D	60 Min Sample 3	13508.60	13508.60	10291.20		83.82
10042050.D	Blank	0.00				
10042051.D	60 Min Sample 1	5557.40	5557.40	4820.10		60.90
10042052.D	Blank	0.00				
10042053.D	60 Min Air Blank	5467.00	5467.00	4762.90		60.28

One microliter suspended water droplets exposed for varying time periods (in Methanol).

File Name	Description	499 Peak Area	Corrected 499 Peak Area	503 Peak Area	RRF	Mass (ng)
10043002.D	Blank	<500				
10043003.D	Calibration Standard	8200.65	12085.7	6685.4	0.68	73.69
10043004.D	Blank	<500				
10043005.D	5 Min Sample 1	208802.2	207846.075	2269.5		3733.02
10043006.D	Blank	502.1				
10043007.D	5 Min Sample 2	256187.3	255231.175	2234.7		4655.47
10043008.D	Blank	1069				
10043009.D	5 Min Sample 3	375809.6	374853.475	3333.6		4583.50
10043010.D	Blank	586.5				
10043011.D	5 Min Blank	<500	--	2728.7		--
10043012.D	Blank	<500				
10043013.D	15 Min Sample 1	18764.7	17808.575	12350.4		112.44
10043014.D	Blank	<500				
10043015.D	15 Min Sample 2	9310.7	8354.575	11476.2		56.77
10043016.D	Blank	<500				
10043017.D	15 Min Sample 3	8017.8	7061.675	11174.8		49.28
10043018.D	Blank	<500				
10043019.D	15 Min Air Blank	600.8	-355.325	10810.50		-2.56
10043020.D	Blank	<500				
10043021.D	Calibration Standard	11636.4	10680.275	18148.40	1.30	45.89
10043022.D	Blank	1305.6				
10043023.D	30 Min Sample 1	14939.6	13983.475	10505.50		103.80
10043024.D	Blank	<500				
10043025.D	30 Min Sample 2	19572.5	18616.375	12315.10		117.88
10043026.D	Blank	<500				
10043027.D	30 Min Sample 3	10754.2	9798.075	11332.70		67.42
10043028.D	Blank	<500				
10043029.D	30 Min Air Blank	1607.98	651.855	23828.80		2.13
10043030.D	Blank	<500				

One microliter suspended water droplets exposed for varying time periods (continued from above).

File Name	Description	499 Peak Area	Corrected 499 Peak Area	503 Peak Area	RRF	Mass (ng)
10043031.D	Calibration Standard	13199.5	12243.375	19410.8	1.23	46.38
10043032.D	Blank	<500				
10043033.D	60 Min Sample 1	23736.2	22780.075	13021.40		128.63
10043034.D	Blank	<500				
10043035.D	60 Min Sample 2	19466	18509.875	14657.00		92.86
10043036.D	Blank	978.5				
10043037.D	60 Min Sample 3	25381.9	24425.775	17887.10		100.41
10043038.D	Blank	1312.2				
10043039.D	60 Min Air Blank	1120.3	164.175	13716.00		0.88
10043040.D	Blank	993.1				
10043041.D	Calibration Standard	13812.6	12856.475	20851.70	1.26	46.54
10043042.D	Blank	902				
Average Blank			956.125			

One microliter suspended water droplets for 5 minutes both with and without PFOS added to the water (in Methanol).

File Name	Description	Corrected Area of 499 Peak	Area of 503 Peak	RRF	Mass of PFOS Observed (ng)
10050902.D	Blank				
10050903.D	Calibration Standard	12085.70	276142.50	1.18	50.00
10050904.D	Blank				
10050905.D	Reg H20 Green 1	15234397.63	143276.90		7496.97
10050906.D	Blank				
10050907.D	Reg H20 Green 2	11443234.63	150434.90		5363.36
10050908.D	Blank				
10050909.D	Reg H20 Green 3	178965.03	147400.30		85.61
10050910.D	Blank				
10050911.D	Reg H20 Air Blank 1	612.83	156929.90		0.28
10050912.D	Blank				
10050913.D	PFC Purple 1	12747349.63	136218.40		7213.85
10050914.D	Blank				
10050915.D	Water Test	35783.73	120250.90		20.98
10050916.D	Blank				
10050917.D	PFC Purple 2	14275397.63	176826.70		6223.34
10050922.D	Blank				
10050923.D	PFC Purple 3	14188276.63	133341.20		8202.54
10050924.D	Blank				
10050925.D	PFC Purple Air Blank	15860.83	132228.50		9.25
10050926.D	Blank				
10050927.D	Calibration Standard	148562.43	229045.60	1.28	50.00

One microliter suspended water droplets for 5 minutes both with and without PFOS added to the water. (continued from above)

File Name	Description	Corrected Area of 499 Peak	Area of 503 Peak	RRF	Mass of PFOS Observed (ng)
10050928.D	Blank				
10050929.D	PFC Yellow 1	11277177.63	118649.60		7326.85
10050930.D	Blank				
10050931.D	PFC Yellow 2	551354.53	131708.30		322.70
10050932.D	Blank				
10050933.D	Reg H20 Yellow 3	12778755.63	112767.00		8735.53
10050934.D	Blank				
10050935.D	3rd Air Blank	801.53	123008.30		0.50
10050936.D	Blank				

Suspended water droplets exposed for 30 minutes, with volume varying from 1-4 µl in Methanol).

File Name	Description	Area of 499 Peak	Corrected Area of 499 Peak	Area of 503 Peak	RRF	PFOS Observed (ng)
10051202.D	Blank	3759.10				
10051203.D	Calibration Standard	189694.20	187214.39	271014.80	1.19	50.00
10051204.D	Blank	5574.10				
10051205.D	1 uL Drop 30 Min (1)	559366.00	556886.19	147965.70		268.85
10051206.D	Blank	2878.80				
10051207.D	1 uL Drop 30 Min (2)	385576.80	383096.99	148243.80		184.60
10051208.D	Blank	2422.00				
10051209.D	1 uL Drop 30 Min (3)	406820.20	404340.39	151191.20		191.04
10051210.D	Blank	2848.10				
10051211.D	1uL Air Blank	13573.40	11093.59	146597.50		5.41
10051212.D	Blank	1722.70				
10051213.D	2 uL Drop 30 Min (1)	106334.30	103854.49	135981.50		57.57
10051214.D	Blank	1941.27				
10051215.D	2 uL Drop 30 Min (2)	78892.40	76412.59	164870.90		34.94
10051216.D	Blank	1914.51				
10051217.D	2 uL Drop 30 Min (3)	128130.20	125650.39	149360.80		63.42
10051218.D	Blank	1459.80				
10051219.D	2 uL Air Blank	11428.60	8948.79	152968.00		4.41
10051220.D	Blank	7072.32				
10051221.D	Calibration Standard	119637.90	117158.09	176638.80	1.26	50.00
10051222.D	Blank	1290.00				
10051223.D	3 uL Drop 30 Min (1)	204131.30	201651.49	158753.70		95.75
10051224.D	Blank	1552.20				
10051225.D	3 uL Drop 30 Min (2)	650412.90	647933.09	184094.10		265.32
10051226.D	Blank	1347.50				
10051227.D	3 uL Drop 30 Min (3)	192198.60	189718.79	161309.70		88.66
10051228.D	Blank	2110.90				

Suspended water droplets exposed for 30 minutes, with volume varying from 1-4 µl (continued from above).

File Name	Description	Corrected Area of 499 Peak	Area of 503 Peak	Realitive Response Factor (RRF)	Mass of PFOS Observed (ng)
10051229.D	3 uL Air Blank	11027.40	8547.59	149377.40	
10051230.D	Blank	2396.35			
10051231.D	Calibration Standard	109456.39	168069.50	1.28	50.00
10051232.D	Blank				
10051233.D	4 uL Drop 30 Min (1)	318457.99	171119.30		137.57
10051234.D	Blank				
10051235.D	4 uL Drop 30 Min (2)	244614.19	139052.30		130.04
10051236.D	Blank				
10051237.D	4 uL Drop 30 Min (3)	304810.69	171980.40		131.02
10051238.D	Blank				
10051239.D	4 uL Air Blank	9162.29	124709.80		5.64
10051240.D	Blank				
10051241.D	Calibration Standard	114214.69	168863.50	1.23	50.00
10051242.D	Blank				
Average Blank	2479.811429				

Suspended water droplets exposed for 60 minutes, with volume varying from 1-4 µl (in methanol).

File Name	Description	Area of 499 Peak	Corrected Area of 499 Peak	Area of 503 Peak	Realitive Response Factor (RRF)	Mass of PFOS Observed (ng)
10051902.D	Blank	4006.4				
10051903.D	Calibration Standard	63633.4	63200.675	89305.8	1.17	50.00
10051904.D	Blank	0				
10051905.D	1 uL Drop 60 Min (1)	80200.4	79767.675	71745.6		78.02
10051906.D	Blank	2639.58				
10051907.D	1 uL Drop 60 Min (2)	174395	173962.27	83809.9		145.65
10051908.D	Blank	2441.25				
10051909.D	1 uL Drop 60 Min (3)	229189	228756.27	115695		138.75
10051910.D	Blank					
10051911.D	1uL Air Blank	7488.9	7056.1748	130425		3.80
10051912.D	Blank					
10051913.D	2 uL Drop 60 Min (1)	222482.3	222049.57	110953		140.44
10051914.D	Blank					
10051915.D	2 uL Drop 60 Min (2)	185032.1	184599.4	111761		115.91
10051916.D	Blank					
10051917.D	2 uL Drop 60 Min (3)	137368.4	136935.67	108987		88.17
10051918.D	Blank					
10051919.D	2 uL Air Blank	10620.1	10187.37	150698		1.41
10051920.D	Blank					
10051921.D	Calibration Standard	219669	219236.27	91462.2	0.35	50.00
10051922.D	Blank					

Suspended water droplets exposed for 60 minutes, with volume varying from 1-4 µl (continued from above).

File Name	Description	Corrected Area of 499 Peak	Area of 503 Peak	Realitive Response Factor (RRF)	Mass of PFOS Observed (ng)
10051923.D	3 uL Drop 60 Min (1)	214648.8	214216.07	113445.6	
10051924.D	Blank				
10051925.D	3 uL Drop 60 Min (2)	179021.7	178588.97	139738.5	
10051926.D	Blank				
10051927.D	3 uL Drop 60 Min (3)	168138.7	167705.97	107442.9	
10051928.D	Blank				
10051929.D	3 uL Air Blank	11869.9	11437.17	115450.8	
10051930.D	Blank				
10051931.D	Calibration Standard	208519.575	94619.5	0.38	50.00
10051932.D	Blank				
10051933.D	4 uL Drop 60 Min (1)	99557.57	118469.4		58.97
10051934.D	Blank				
10051935.D	4 uL Drop 60 Min (2)	26750.57	158633.7		11.83
10051936.D	Blank				
10051937.D	4 uL Drop 60 Min (3)	114982.07	117332.5		68.77
10051938.D	Blank				
10051939.D	4 uL Air Blank	8041.07	101004.9		1.81
10051940.D	Blank				
10051941.D	Calibration Standard	213895.27	97828.7	0.38	50.00